DESY 14-109

CP violation in bilinear R-parity violation and its consequences for the early universe

Asma Chériguène[a], Stefan Liebler[b], Werner Porod[a]

[a] *Institut für Theoretische Physik und Astrophysik, Universität Würzburg 97074 Würzburg, Germany*

[b] *II. Institut für Theoretische Physik, Universität Hamburg 22761 Hamburg, Germany*

Abstract

Supersymmetric models with bilinear R-parity violation (BRpV) provide a framework for neutrino masses and mixing angles to explain neutrino oscillation data. We consider CP violation within the new physical phases in BRpV and discuss their effect on the generation of neutrino masses and the decays of the lightest supersymmetric particle (LSP), being a light neutralino with mass $\sim 100\,\text{GeV}$, at next-to-leading order. The decays affect the lepton and via sphaleron transitions the baryon asymmetry in the early universe. For a rather light LSP, asymmetries generated before the electroweak phase transition via e.g. the Affleck-Dine mechanism are reduced up to two orders of magnitude, but are still present. On the other hand, the decays of a light LSP themselves can account for the generation of a lepton and baryon asymmetry, the latter in accordance to the observation in our universe, since the smallness of the BRpV parameters allows for an out-of-equilibrium decay and sufficiently large CP violation is possible consistent with experimental bounds from the non-observation of electric dipole-moments.

1 Introduction

The observed baryonic component of the universe comes along with the question why the universe consists of entirely matter with hardly any primordial antimatter [1]. Defining the baryon and antibaryon number density n_B and $n_{\bar{B}}$ and the entropy s at temperature T, the baryon asymmetry can be expressed in terms of the quantity

$$\delta_B = \frac{n_B - n_{\bar{B}}}{s} \quad . \tag{1}$$

The value of δ_B, which is consistent with the primordial abundances of light elements originating from big bang nucleosynthesis [2, 3], is $\delta_B = (6.19 \pm 0.14) \cdot 10^{-10}$ extracted from the measurements of the acoustic peaks in the cosmic microwave background (CMB) [4, 5].

The dynamical creation of the baryon asymmetry in the universe (Baryogenesis) requires the implementation of the three Sakharov conditions [6]: violation of baryon number B, C symmetry and CP symmetry violation and departure from thermal equilibrium. Nonperturbative effects (sphalerons) [7] can give rise to processes, which conserve $B-L$ with L being the lepton number of involved particles, but violate $B+L$. Thus, a generated lepton asymmetry can account for the observed baryon asymmetry as well (Baryogenesis via Leptogenesis [8–10]), in particular since lepton asymmetries are hardly constrained by experiments [11–13].

In bilinear R-parity violation, where L violating parameters allow for the generation of neutrino masses and mixing, the decays of the lightest supersymmetric particle (LSP) can thus affect the lepton and baryon asymmetries in the early universe after inflation. Whereas L violation is explicitly given by the BRpV parameters, we incorporate CP violation by complex phases for those parameters. Lastly, the LSP decay widths are small enough to be out of equilibrium, if the BRpV parameters are chosen in agreement with neutrino masses and mixing and the LSP is rather light, e.g. $m_{\tilde{\chi}_1^0} \lesssim 100$ GeV. We study the evolution of the number densities by solving numerically the corresponding Boltzmann equations. On the one hand existing asymmetries e.g. induced by the Affleck-Dine mechanism [14] are reduced by up to two orders of magnitude, but are still present. On the other hand we demonstrate that CP violating LSP decays can generate lepton asymmetries. Before the electroweak phase transition the latter asymmetries can be partially transferred to baryon asymmetries via sphaleron transitions in accordance to the observation.

Earlier works on Leptogenesis in the context of BRpV [15–19] made use of complex gaugino masses, leaving the R-parity violating parameters real. In those cases only small lepton asymmetries below 10^{-10} can be generated, if the LSP is supposed to decay out of equilibrium. However, nonholomorphic terms in combination with fixed particle spectra [16] induce small enough decay widths for the neutralino to be out of equilibrium and allow for large enough CP asymmetries in the decay products being a charged Higgs boson and a lepton. As it was pointed in Ref. [15] lepton number violating decays can also spoil existing lepton asymmetries.

We focus on BRpV parameters, which are in agreement with the observations of neutrino oscillations. In accordance to the global fit carried out in Refs. [20–23] the preferred and in our analysis employed ranges of the oscillation parameters at 2σ (for a normal neutrino mass

hierarchy) are given by Ref. [22] [1]

$$\begin{aligned} 0.376 \leq &\sin^2\theta_{23} \leq 0.506 \ , \qquad 2.30\times10^{-3}\ \text{eV}^2 \leq \Delta m^2_{31} \leq 2.59\times10^{-3}\ \text{eV}^2 \\ 0.275 \leq &\sin^2\theta_{12} \leq 0.342 \ , \qquad 7.15\times10^{-5}\ \text{eV}^2 \leq \Delta m^2_{21} \leq 8.00\times10^{-5}\ \text{eV}^2 \\ 0.0197 \leq &\sin^2\theta_{13} \leq 0.0276 \quad . \end{aligned} \tag{2}$$

The explanation of neutrino masses and mixing within BRpV was widely discussed in the literature, for reviews we refer to Refs. [24–26]. In BRpV it is well-known that lowest order in perturbation theory is not sufficient to generate the full neutrino spectrum, however loop corrections can nicely explain the mass hierarchy between the neutrino mass eigenstates [27–37]. We shortly repeat the discussion, but focus mainly on complex phases in the BRpV parameters, which additionally induce a Dirac CP phase in the lepton/neutrino mixing matrix. CP violation in the partial decay widths of the LSP occurs at the one-loop level [38]. Our calculation of LSP decays at next-to-leading order (NLO) is based on Refs. [39, 40].

The remainder of this paper is organized as follows: In Sect. 2 we explain the theory behind BRpV for complex BRpV parameters. This discussion includes the generation of neutrino masses and the calculation of the LSP decay at NLO in the electromagnetic coupling. Moreover we provide the basics of number density evolution in the early universe by the introduction of Boltzmann equations. Afterwards we shortly present a simple description of the transition between a lepton and baryon asymmetry via sphaleron transitions. In Sect. 3 we show our numerical results starting again with neutrino masses and mixing and the neutralino decays. In case of CP conserving BRpV initial asymmetries can be reduced, being up to two orders of magnitude lesser in size. For CP violation instead the neutralino decays themselves provide a large lepton asymmetry, which is partially transformed to a baryon asymmetry due to sphaleron transitions. In the last subsection we elaborate on the effects of LSP annihilation to SM particles in more detail. Finally we conclude in Sect. 4 and present the implemented Boltzmann equations in the Appendix.

2 Bilinear R-parity violation and CP violation therein

For bilinear R-parity violation (BRpV), which was first discussed in Refs. [41–45], the superpotential is given by

$$W \ = \ \varepsilon_{ab}[Y_U^{ij}\hat{Q}_i^a\hat{U}_j^c\hat{H}_u^b + Y_D^{ij}\hat{Q}_i^b\hat{D}_j^c\hat{H}_d^a + Y_E^{ij}\hat{L}_i^b\hat{E}_j^c\hat{H}_d^a - \mu\hat{H}_d^a\hat{H}_u^b + \epsilon_i\hat{L}_i^a\hat{H}_u^b] \quad , \tag{3}$$

where Y_U, Y_D and Y_E are the (3×3) Yukawa matrices and $\varepsilon_{\alpha\beta}$ is the complete antisymmetric SU(2) tensor with $\varepsilon_{12}=1$, whereas i,j denote the three generations of leptons and quarks. The last terms ϵ_i explicitly break lepton number L and are similar to the parameter μ, which determines the mass of the Higgsinos, given in units of mass. Additionally the three soft-SUSY breaking parameters B_i are added to the minimal supersymmetric standard model (MSSM)

[1] Similar values are found by the most recent global fit in Ref. [23].

soft-breaking Lagrangian

$$\begin{aligned}\mathcal{L}_{soft} &= M_Q^{ij2}\tilde{Q}_i^{a*}\tilde{Q}_j^a + M_U^{ij2}\tilde{U}_i\tilde{U}_j^* + M_D^{ij2}\tilde{D}_i\tilde{D}_j^* + M_L^{ij2}\tilde{L}_i^{a*}\tilde{L}_j^a + M_E^{ij2}\tilde{E}_i\tilde{E}_j^* \\ &+ m_{H_d}^2 H_d^{a*}H_d^a + m_{H_u}^2 H_u^{a*}H_u^a - \frac{1}{2}\Big[M_1\tilde{B}^0\tilde{B}^0 + M_2\tilde{W}^\gamma\tilde{W}^\gamma + M_3\tilde{g}^{\gamma'}\tilde{g}^{\gamma'} + h.c.\Big] \\ &+ \varepsilon_{ab}\Big[T_U^{ij}\tilde{Q}_i^a\tilde{U}_j^* H_u^b + T_D^{ij}\tilde{Q}_i^b\hat{D}_j^* H_d^a + T_E^{ij}\tilde{L}_i^b\tilde{E}_j^* H_d^a - B_\mu\mu H_d^a H_u^b - B_i\epsilon_i\tilde{L}_i^a H_u^b + h.c.\Big], \quad (4)\end{aligned}$$

where a summation over $a, b \in \{1, 2\}$, $\gamma \in \{1, 2, 3\}$ and $\gamma' \in \{1, \ldots, 8\}$ and the generation indices i and j is implied. The vacuum structure induces vacuum expectation values (VEVs) for the neutral components of the Higgs fields $\langle H_u^0\rangle = v_u/\sqrt{2}$ and $\langle H_d^0\rangle = v_d/\sqrt{2}$ as well as the sneutrinos $\langle\tilde{\nu}_i\rangle = v_i/\sqrt{2}$. The latter VEVs together with the last term in Eq. (3) result in a mixing between the gauge eigenstates of the neutralinos $\tilde{B}$, $\tilde{W}_3^0$, $\tilde{H}_d^0$ and $\tilde{H}_u^0$ and the three left-handed neutrinos ν_i at tree-level, providing an effective Majorana mass term for the neutrinos at tree-level [32, 36, 46]. Moreover the charginos mix with the charged leptons and the scalars, pseudoscalars and charged scalar states have to be combined with the sneutrinos and sleptons respectively.

To study the effects of CP violation in BRpV we closely follow Ref. [38] and allow for complex parameters

$$\epsilon_i = \epsilon_i^R + i\epsilon_i^I, \quad B_i = B_i^R + iB_i^I, \quad B_\mu = B_\mu^R + iB_\mu^I \quad (5)$$

in the superpotential Eq. (3) and the soft-breaking terms in Eq. (4). Our phase convention is such that the gaugino mass parameter M_2 is real and positive. To simplify our model, μ and all other parameters in the soft-breaking Lagrangian are taken to be real, although additional complex phases are possible. In this way, the constraints on the electric dipole-moments of electron, neutron and various atoms are satisfied if the parameters are chosen to fulfill neutrino data [38]. In case of CP violation scalars and pseudoscalars are indistinguishable. The resulting mass matrix is shown in Ref. [38]. We choose the VEVs v_d, v_u and v_i to be real and determine the real and complex parts of B_μ and B_i from the tadpole equations. Due to the real μ parameter it yields $B_\mu^I \propto \sum_i v_i\epsilon_i^I$ and $B_i^I \propto \epsilon_i^I$, such that the real BRpV model is restored in the limit $\epsilon_i^I \to 0$.

2.1 Neutrino masses and mixing angles

In this subsection we discuss the neutralino sector of BRpV at tree-level. We refer to Refs. [27–37, 40] for studies related to neutrino masses in bilinear R-parity violation. If we make use of the basis

$$\left(\psi^0\right)^T = \left(\tilde{B}^0, \tilde{W}_3^0, \tilde{H}_d^0, \tilde{H}_u^0, \nu_1, \nu_2, \nu_3\right) \quad (6)$$

the mass matrices of the neutral fermions have the generic form

$$\mathcal{M}_n^{\text{tree}} = \begin{pmatrix} M_H & \hat{m} \\ \hat{m}^T & 0 \end{pmatrix} \quad (7)$$

and enter the Lagrangian density as follows

$$\mathcal{L} \supset -\frac{1}{2}\left((\psi^0)^T\mathcal{M}_n^{\text{tree}}\psi^0\right) - \frac{1}{2}\left((\psi^0)^\dagger\mathcal{M}_n^{\text{tree}*}\psi^{0*}\right) \quad . \quad (8)$$

Therein the sub-matrix M_H is the usual MSSM neutralino mass matrix, whereas the sub-matrix $\hat{m}$ includes the mixing with the left-handed neutrinos and contains the R-parity violating parameters. In detail the elements are

$$M_H = \begin{pmatrix} M_1 & 0 & -\frac{1}{2}g'v_d & \frac{1}{2}g'v_u \\ 0 & M_2 & \frac{1}{2}gv_d & -\frac{1}{2}gv_u \\ -\frac{1}{2}g'v_d & \frac{1}{2}gv_d & 0 & -\mu \\ \frac{1}{2}g'v_u & -\frac{1}{2}gv_u & -\mu & 0 \end{pmatrix}, \quad \hat{m}^T = \begin{pmatrix} -\frac{1}{2}g'v_1 & \frac{1}{2}gv_1 & 0 & \epsilon_1 \\ -\frac{1}{2}g'v_2 & \frac{1}{2}gv_2 & 0 & \epsilon_2 \\ -\frac{1}{2}g'v_3 & \frac{1}{2}gv_3 & 0 & \epsilon_3 \end{pmatrix} \tag{9}$$

with g and g' being the gauge couplings of $SU(2)_L$ and $U(1)_Y$ respectively. The mass eigenstates F_i^0 are related to the gauge eigenstates ψ_s^0 by $F_i^0 = \mathcal{N}_{is}\psi_s^0$, where the unitary matrix $\mathcal{N}$ diagonalizes the full neutralino mass matrix $\mathcal{M}_n$ in accordance to

$$\mathcal{M}_{n,dia.} = \text{Diag}\left(m_{\tilde{\chi}_1^0}, \ldots, m_{\tilde{\chi}_7^0}\right) = \mathcal{N}^* \mathcal{M}_n^{\text{tree}} \mathcal{N}^\dagger \quad , \tag{10}$$

The second part of the Lagrangian density in Eq. (8) has to be diagonalized by $\mathcal{N}\mathcal{M}_n^{\text{tree}*}\mathcal{N}^T$ in case of CP violation. The mass eigenstates in Weyl notation can finally be build up to 4-component spinors by

$$\tilde{\chi}_i^0 = \begin{pmatrix} F_i^0 \\ F_i^{0\dagger} \end{pmatrix} \quad . \tag{11}$$

The mixing of neutrinos with neutralinos gives rise to one massive neutrino at tree-level. Its mass yields

$$m_{\nu_3} = \frac{g^2 M_1 + g'^2 M_2}{4\text{det}(M_H)} |\vec{\Lambda}|^2 \quad , \tag{12}$$

with the alignment parameter $\Lambda_i = \mu v_i + \epsilon_i v_d$. The atmospheric and the reactor mixing angle of the neutrinos can be expressed in terms of the alignment parameters Λ_i at tree-level by

$$\tan^2\theta_{23} = \left|\frac{\Lambda_2}{\Lambda_3}\right|^2, \qquad |U_{e3}|^2 \simeq \frac{|\Lambda_1|^2}{|\Lambda_2|^2 + |\Lambda_3|^2} \quad . \tag{13}$$

At one-loop level $|U_{e3}|$ can receive considerable corrections. In the complex case the absolute value of Λ_i is given by $|\Lambda_i|^2 = |\mu v_i + v_d \epsilon_i^R|^2 + |v_d \epsilon_i^I|^2$. Necessarily the size of $|\epsilon_i^I| \sim |\Lambda_i|/v_d$ is fixed by the neutrino mass generated at tree-level as shown in Eq. (12) and needs to be smaller than the value of ϵ_i^R in the pure real case, where a cancellation between the two terms of Λ_i can be arranged. As a consequence neutrino data will restrict the size of possible complex phases $\phi_i = \arctan(\epsilon_i^I/\epsilon_i^R)$. This observation is in accordance to the discussion in Ref. [38], where the cancellation between the terms within Λ_i is used to constrain the complex phases. Setting the complex phase of M_2 to zero allows for a phase ϕ_μ for the μ parameter, which in turn permits larger complex phases for the parameters ϵ_i. However, ϕ_μ is severely constrained by the non-observation of electric dipole-moments and within the allowed range for ϕ_μ the impact of this phase is small and does not lead to any new qualitative features.

In the following we discuss the effects of NLO corrections to the neutralino mass matrix, which allow for the explanation of the solar mass and mixing angle in accordance to Ref. [22] as well. Compared to existing work [27–37, 40] we define $\overline{\text{DR}}$ masses at NLO for the neutralino and

neutrino sector in a slightly different way which is better suited for the study of CP violating effects. The fermionic self-energies can be decomposed as follows

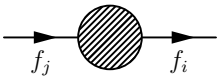

$$\equiv \Gamma_{ij} = \delta_{ij}(\not{p} - m_{fi}) + \Big[\not{p}\left(P_L\hat{\Sigma}^L_{ij}\left(p^2\right) + P_R\hat{\Sigma}^R_{ij}\left(p^2\right)\right) + P_L\hat{\Sigma}^{SL}_{ij}(p^2) + P_R\hat{\Sigma}^{SR}_{ij}(p^2)\Big] \quad , \tag{14}$$

where the hat refers to $\overline{\text{DR}}$ renormalized contributions and $P_{L,R} = \frac{1}{2}(1 \mp \gamma_5)$ are projection operators. They enter the Lagrangian density in the form $-\frac{1}{2}\overline{\tilde{\chi}}^0_i\Gamma_{ij}\tilde{\chi}^0_j$ including both terms of Eq. (8). In order to calculate $\overline{\text{DR}}$ masses for the neutralinos, we have to respect that F_i and F_i^* are obtained from gauge eigenstates by $\mathcal{N}$ and $\mathcal{N}^*$ respectively. Taking the different rotations into account we define the $\overline{\text{DR}}$ mass term to be added at NLO by

$$\mathcal{M}_n^{\text{tree}} \to \mathcal{M}_n^{\text{tree}} - \delta\mathcal{M}_n \qquad \text{with} \tag{15}$$

$$(\delta\mathcal{M}_n)_{ij}\left(p^2\right) = \sum_k \frac{1}{2}(\mathcal{M}_n^{\text{tree}})_{ik}(\mathcal{N}^\dagger\hat{\Sigma}^{R,T}(p^2)\mathcal{N})_{kj} + \frac{1}{2}(\mathcal{N}^T\hat{\Sigma}^R(p^2)\mathcal{N}^*)_{ik}(\mathcal{M}_n^{\text{tree}})_{kj} + \frac{1}{2}(\mathcal{N}^T\hat{\Sigma}^{SL,T}(p^2)\mathcal{N})_{ij} + \frac{1}{2}(\mathcal{N}^T\hat{\Sigma}^{SL}(p^2)\mathcal{N})_{ij} \tag{16}$$

As we are dealing with Majorana particles, one finds

$$\Sigma^L_{ij}(p^2) = \Sigma^R_{ji}(p^2), \qquad \Sigma^{SL}_{ij}(p^2) = \Sigma^{SL}_{ji}(p^2), \qquad \Sigma^{SR}_{ij}(p^2) = \Sigma^{SR}_{ji}(p^2) \tag{17}$$

such that we are able to rewrite Eq. (16)

$$(\delta\mathcal{M}_n)_{ij}\left(p^2\right) = \sum_k \frac{1}{2}(\mathcal{M}_n^{\text{tree}})_{ik}(\mathcal{N}^\dagger\hat{\Sigma}^L(p^2)\mathcal{N})_{kj} + \frac{1}{2}(\mathcal{N}^T\hat{\Sigma}^R(p^2)\mathcal{N}^*)_{ik}(\mathcal{M}_n^{\text{tree}})_{kj} + (\mathcal{N}^T\hat{\Sigma}^{SL}(p^2)\mathcal{N})_{ij} \quad . \tag{18}$$

Therein we perform the following replacement for the practical calculation

$$\hat{\Sigma}_{ij}(p^2) \to \frac{1}{2}(\hat{\Sigma}_{ij}(m_i^2) + \hat{\Sigma}_{ij}(m_j^2)) \quad . \tag{19}$$

Eq. (18) is similar to the formulas in Refs. [47,48], generalized for the left-hand part of Eq. (8). Adding the Goldstone tadpoles as done in Refs. [32, 39, 40] allows for the determination of gauge-independent neutralino/neutrino masses at NLO. In principle the generalization of the on-shell neutralino and neutrino masses as shown in Ref. [40] is straightforward, but will not be presented in this context. Rather we point out the most important NLO contributions in the following: For large values of $\tan\beta$ b-(s)quark contributions are of quite importance. However, a major contribution always stems from loops involving a neutral or charged scalar, whereas loops with gauge bosons are less dominant.

The unitary matrix $\mathcal{N}$, which diagonalizes the neutralino mass matrix, contains the block mixing the neutrino generations, which together with the leptonic block in the chargino mixing matrices, forms the Pontecorvo-Maki-Nakagawa-Sakata matrix (PMNS) $U^{l\nu}$ matrix [49].

The latter contains at least one CP violating phase, namely the Dirac phase δ, which enters the Jarlskog invariant [50] in the lepton/neutrino sector as follows

$$J_{\rm CP} = {\rm Im}(U_{23}^{l\nu} U_{13}^{l\nu *} U_{12}^{l\nu} U_{22}^{l\nu *}) = \frac{1}{8} \cos\theta_{13} \sin(2\theta_{12}) \sin(2\theta_{23}) \sin(2\theta_{13}) \sin\delta \quad . \tag{20}$$

We will demonstrate in Sect. 3.1 that in our restricted range of phases $|J_{\rm CP}|$ can be sizable and close to the experimental bound.

2.2 Leptonic neutralino decays

We turn to the calculation of the decays of the lightest neutralino, which are dominated by L violating two-body decays for neutralino masses above m_W. We follow Refs. [39, 40] regarding the evaluation of the decay widths. Even though the loop contributions, which generate eventually the lepton asymmetry, are finite, we do perform a complete one-loop analysis to ensure that the life-time remains long enough such that the neutralino decays out of equilibrium. We start with a short discussion of the LO decay width, for which the relevant part of the Lagrangian density is given by

$$\begin{aligned} \mathcal{L} \supset & \overline{\tilde{\chi}_l^0} \gamma^\mu \left(P_L O_{Llj}^Z + P_R O_{Rlj}^Z \right) \tilde{\chi}_j^0 Z_\mu + \left(\overline{\tilde{\chi}_l^-} \gamma^\mu \left(P_L O_{Llj}^W + P_R O_{Rlj}^W \right) \tilde{\chi}_j^0 W_\mu^- + \text{h.c.} \right) \\ & + \overline{\tilde{\chi}_l^0} (P_L O_{Llj}^{h^0} + P_R O_{Rlj}^{h^0}) \tilde{\chi}_j^0 h^0 \quad . \end{aligned} \tag{21}$$

It includes the coupling to the charged leptons $l^\pm$, which are part of the charginos $\tilde{\chi}_l^\pm$. The explicit form of the couplings can be taken from Ref. [40]. The widths for the channels involving a final state gauge boson can be written as follows

$$\Gamma^0 = \frac{\sqrt{\kappa(m_i^2, m_o^2, m_V^2)}}{16\pi m_i^3} \left[\left(|O_L^V|^2 + |O_R^V|^2 \right) f(m_i^2, m_o^2, m_V^2) - 6{\rm Re}(O_L^V O_R^{V*}) m_i m_o \right] \tag{22}$$

with $V \in \{W, Z\}$, the masses of the mother (daughter) particle m_i (m_o) and the functions

$$f(x,y,z) = \frac{x+y}{2} - z + \frac{(x-y)^2}{2z}, \quad \kappa(x,y,z) = x^2 + y^2 + z^2 - 2xy - 2xz - 2yz \quad . \tag{23}$$

In case of the channel with a final state Higgs boson the partial width is given by

$$\Gamma^0 = \frac{\sqrt{\kappa(m_i^2, m_o^2, m_h^2)}}{16\pi m_i^3} \left[\frac{|O_L^{h^0}|^2 + |O_R^{h^0}|^2}{2} (m_i^2 + m_o^2 - m_h^2) + 2{\rm Re}(O_L^{h^0} O_R^{h^0 *}) m_i m_o \right] . \tag{24}$$

The LO decay widths with leptons/neutrinos and antileptons/antineutrinos in the final state are identical. In order to observe CP violating effects with respect to the different final states we proceed as in Refs. [39, 40] and calculate NLO contributions, which are all implemented in `CNNDecays`. The NLO decay widths can be written in the form

$$\Gamma^1 = \Gamma^0 + \frac{\sqrt{\kappa(m_i^2, m_o^2, m_V^2)}}{16\pi m_i^3} \frac{1}{2} \sum_{\rm pol} 2{\rm Re} \left({\rm M}_1 {\rm M}_0^\dagger \right) \tag{25}$$

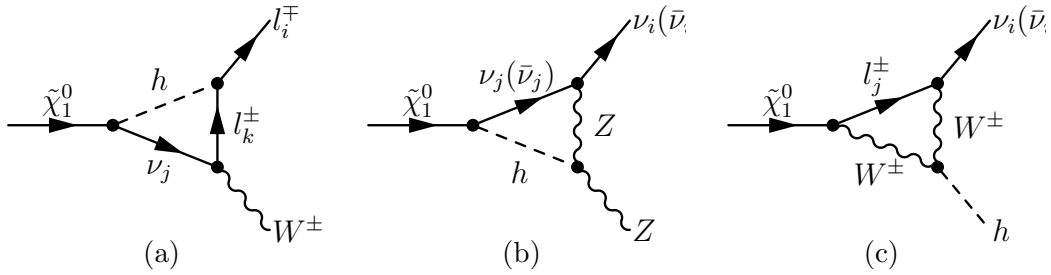

Figure 1: Dominant NLO virtual contribution generating a CP asymmetry between the different final states for (a) $\tilde{\chi}_1^0 \to l^\pm W^\mp$; (b) $\tilde{\chi}_1^0 \to \nu Z$; (c) $\tilde{\chi}_1^0 \to \nu h$.

with the tree-level amplitude M_0 and the NLO amplitude M_1. The latter includes the NLO vertex corrections as well as the wavefunction corrections of in- and outgoing particles as discussed in Refs. [39,40]. For the decay $\tilde{\chi}_1^0 \to l^\pm W^\mp$ real corrections by photon emission are added accordingly. For $\tilde{\chi}_1^0 \to \nu(\overline{\nu})Z$ we distinguish neutrinos and antineutrinos as follows: We assign a lepton number $+1(-1)$ to the left-handed (right-handed) part of the neutrino Dirac spinor, which due to the smallness of neutrino masses and the energies considered here is an extremely good approximation. For LSP masses above the lightest Higgs mass the decay channel $\tilde{\chi}_1^0 \to \nu(\bar{\nu})h$ is relevant as well. We implemented the NLO virtual contributions for the latter decays to `CNNDecays` in order to estimate the CP asymmetry with respect to the different final states and find a similar asymmetry as in the decays involving heavy gauge boson final states.

In Fig. 1 we show the dominant NLO virtual contributions, which generate the CP asymmetry between the final states $l^- W^+$ and $l^+ W^-$ in accordance to Ref. [38], νZ and $\bar{\nu} Z$ as well as νh and $\bar{\nu} h$. In case of a light stau, the corresponding light stau loop contribution to final states containing a (anti-)neutrino could be as important as the ones shown.

2.3 Number density evolution via Boltzmann equations

Within this section we present the evolution of number densities in the universe at temperatures which correspond to energies around the electroweak scale. For a quantitative discussion we make use of Boltzmann equations, in which we take into account the decays as well as the inverse decays of the lightest neutralino. Moreover we add R-parity conserving annihilation processes of the LSP, which are known to have an impact on the final particle densities [17]. Sphaleron transitions between baryon and lepton asymmetries are discussed in Sect. 2.4. However, we can neglect R-parity violating scattering processes changing the lepton number by one or two units, since those processes involve an intermediate neutrino or neutralino and are thus either suppressed by the small neutrino mass or a product of R-parity violating couplings. In addition CP violating scatterings affect final particle densities only slightly, if the neutralino density stays close to its equilibrium density as pointed out in

Ref. [51]. Thus, the Boltzmann equations take the generic form

$$xH(x)\frac{dN_{\tilde{\chi}_1^0}}{dx} = -\sum_{i,j}\Big[\frac{\mathrm{K}_1(x)}{\mathrm{K}_2(x)}\Big(N_{\tilde{\chi}_1^0}\Gamma(\tilde{\chi}_1^0\to ij) - \frac{N_iN_j}{N_i^{eq}N_j^{eq}}N_{\tilde{\chi}_1^0}^{eq}\Gamma(ij\to\tilde{\chi}_1^0)\Big) + \hat{\sigma}(\tilde{\chi}_1^0\tilde{\chi}_1^0\to ij)\Big(N_{\tilde{\chi}_1^0}^2 - \frac{N_iN_j}{N_i^{eq}N_j^{eq}}N_{\tilde{\chi}_1^0}^{eq,2}\Big)\Big] \quad , \tag{26}$$

where i,j denote SM particles. $\mathrm{K}_1(x)$ and $\mathrm{K}_2(x)$ are modified Bessel functions, the parameter $x = m_{\tilde{\chi}_1^0}/\mathrm{T}$ denotes the inverse of the temperature and Γ is the usual decay width in the rest frame of the decaying particle.[2] Moreover we define the density $N_i := N_i(x) = n_i(x)/s(x)$ per co-moving volume element by the ratio of the particle density $n_i(x)$ to the entropy $s(x)$. The quantity $\hat{\sigma}$ contains the thermally averaged annihilation cross section $\langle\sigma_{ij}v\rangle$ of the LSP [52]

$$\hat{\sigma}(\tilde{\chi}_1^0\tilde{\chi}_1^0\to ij) = xH(x)\frac{m_{\tilde{\chi}_1^0}}{x^2}\sqrt{\frac{\pi g_*}{45}}M_p\langle\sigma_{ij}v\rangle \quad \text{with} \quad H := H(x) = \sqrt{\frac{4\pi^3 g_*}{45}}\frac{m_{\tilde{\chi}_1^0}^2}{M_p}\frac{1}{x^2} \quad . \tag{27}$$

The latter formulas include the Planck mass M_p and the effective degrees of freedom g_*, which are taken as a function of x from the tabulated values in `micrOMEGAs` [53]. The thermally averaged cross section $\langle\sigma_{ij}v\rangle$ can be calculated with the help of `micrOMEGAs` as the R-parity violating parameters are too small to impact on the MSSM annihilation cross sections.

Since on cosmological timescales the massive gauge bosons and the Higgs boson decay instantaneously, we directly elaborate the Boltzmann equations with the decay products, which assumes the validity of the narrow-width approximation. In turn Eq. (26) can be written in the form

$$\begin{aligned} xH\frac{dN_{\tilde{\chi}_1^0}}{dx} =& -\frac{\mathrm{K}_1(x)}{\mathrm{K}_2(x)}\sum_{i,q,\bar{q}}\Big[N_{\tilde{\chi}_1^0}\Gamma(\tilde{\chi}_1^0\to\bar{\nu}_iZ)\mathrm{Br}(Z\to q\bar{q}) \\ &- \frac{N_{\bar{\nu}_i}}{N_\nu^{eq}}\frac{N_qN_{\bar{q}}}{N_q^{eq}N_q^{eq}}N_{\tilde{\chi}_1^0}^{eq}\Gamma(\bar{\nu}_iZ\to\tilde{\chi}_1^0)\mathrm{Br}(Z\to q\bar{q}) + \dots\Big] \\ &- \sum_{q,\bar{q}}\Big[\hat{\sigma}(\tilde{\chi}_1^0\tilde{\chi}_1^0\to q\bar{q})(N_{\tilde{\chi}_1^0}^2 - \frac{N_qN_{\bar{q}}}{N_q^{eq}N_q^{eq}}N_{\tilde{\chi}_1^0}^{eq2})\Big] + \dots \quad , \end{aligned} \tag{28}$$

where we have just presented the decay of the heavy gauge boson to a quark pair in combination with the LSP annihilation process to this specific final state. The complete set of formulae is given in Appendix A. To shorten our notation we sum up the generations of u- and d-type quarks and denote them q_1 and q_2 in our study. The Boltzmann equations for the number densities of the (anti-)leptons, (anti-)neutrinos and (anti-)quarks are obtained similarly and presented in Appendix A as well.

2.4 Baryogenesis via Leptogenesis

The lepton asymmetry can be transformed into a baryon asymmetry and vice versa via sphaleron transitions [9, 10, 17]. However, the sphaleron rate is dramatically suppressed for

[2] We are using units where the Boltzmann constant k_B is set to 1.

temperatures below the electroweak scale, thus after the electroweak phase transition. We follow Refs. [54,55], which discuss the sphaleron rate in the light of the recent Higgs discovery with $m_H \sim 125\,\text{GeV}$ leading to a critical temperature of $T_c = 159 \pm 1\,\text{GeV}$. Due to the fast drop of the sphaleron rate for temperatures below T_c, we can safely assume that the baryon asymmetry decouples from the lepton asymmetry at this temperature. Effects resulting from the transition region down to temperatures of $m_{\tilde{\chi}_1^0} \sim 100\,\text{GeV}$ are tiny with respect to our qualitative discussion. Nonetheless we implemented formulas (1.10) and (1.11) of Ref. [54] and split them accordingly to particles and antiparticles. For this purpose we define the lepton asymmetry δ_N as sum over neutrino and lepton flavors by

$$\delta_N = \sum_{i=1,2,3} N_{l_i^-} - N_{l_i^+} + N_{\nu_i} - N_{\bar{\nu}_i} \tag{29}$$

and accordingly the baryon asymmetry in the form

$$\delta_B = N_{q_1} - N_{\bar{q}_1} + N_{q_2} - N_{\bar{q}_2} \quad . \tag{30}$$

Formulas (1.10) and (1.11) of Ref. [54] then read e.g.

$$xH\frac{d(N_{q_1} - N_{\bar{q}_1})}{dx} = \frac{\gamma(x)}{2}[\delta_B + \eta(x)\delta_N], \quad xH\frac{d(N_{l_i^-} - N_{l_i^+})}{dx} = \frac{\gamma(x)}{6}[\delta_B + \eta(x)\delta_N]. \tag{31}$$

The function $\gamma(x)$ incorporates the strength of the sphaleron transitions and thus drops rapidly to zero for $T < T_c$, i.e. $x > m_{\tilde{\chi}_1^0}/T_c$. The function $\eta(x)$ determines the ratio of δ_B and δ_N for $x < T_c/m_{\tilde{\chi}_1^0}$. We use $\eta(x) = 0.5$, which is a reasonable approximation for our study. The corresponding results of this procedure are presented in Sect. 3.4.

3 Numerical results

In this section we show numerical results obtained with the previously discussed formulas and tools. We first stick to the CP conserving case of BRpV, before discussing the effects of CP violation on lepton asymmetries and baryon asymmetries in the early universe. Our discussion is based on the following low-energy SUSY points: The soft-breaking masses are set diagonal to $M_L = M_E = 1$ TeV and $M_Q = M_U = M_D = 1.5$ TeV (generation independent) and the gaugino masses are fixed to $M_1 = 100$ GeV, $M_2 = 400$ GeV, $M_3 = 1.5$ TeV, which also ensures compatibility with the latest ATLAS results [56]. We choose the soft-breaking couplings to be $A_b = -1$ TeV and $A_\tau = -500$ GeV. We finally define two points with small and large value of $\tan\beta$, namely:

$$\text{Scenario } P_1\text{: } \tan\beta = 5\,,\ A_t = 3\,\text{TeV} \text{ and Scenario } P_2\text{: } \tan\beta = 35\,,\ A_t = 2.5\,\text{TeV} \tag{32}$$

Similar to the lepton sector the soft-breaking masses of the squark sector are set diagonal. In both cases we set $\mu = 1$ TeV and $m_A = 370$ GeV resulting in a lightest SM-like Higgs h with mass m_h close to 125 GeV and a lightest neutralino with mass close to 105 GeV[3].

[3]For completeness we note, that we have calculated the Higgs masses in the R-parity conserving limit including 2-loop effects using `SPheno` [57,58] as the complete formulae for the Higgs masses including R-parity violation are not known. However, this is an excellent approximation as the corresponding couplings are much smaller than the R-parity conserving ones.

3.1 Neutrino masses and mixing angles

Neutrino data provides a constraint on the possible phases of the parameters ϵ_i, which can be easily understood by $|\Lambda_i|^2 = |\mu v_i + v_d \epsilon_i^R|^2 + |v_d \epsilon_i^I|^2$. As discussed in Sect. 2.1 in the real BRpV a cancellation in the sum $\mu v_i + v_d \epsilon_i$ allows to explain the atmospheric neutrino mass scale at tree-level on the one hand side together with an explanation of the solar mass scale at the loop level thanks to sufficiently large ϵ_i on the other hand [32, 36]. As a consequence purely imaginary ϵ_i for all generations at the same time are impossible. Moreover as v_d decreases with increasing $\tan\beta$ we expect that larger phases are possible for larger values of $\tan\beta$.

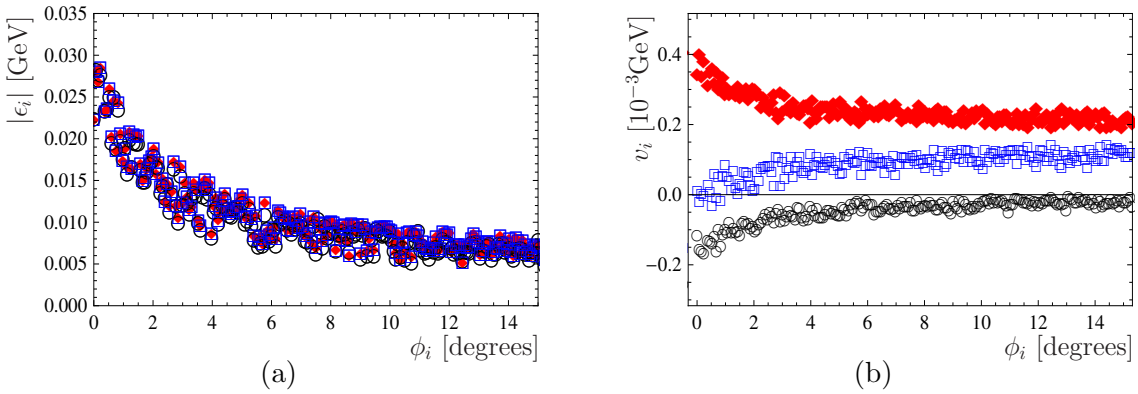

Figure 2: Values of R-parity violating parameters as a function of $\phi := \phi_1 = \phi_2 = \phi_3$ in degrees for scenario P_2, where in (a) we give $|\epsilon_i|$ in GeV with $i = 1$ (black, circle), 2 (blue, square) and 3 (red, diamond) and in (b) v_i in 10^{-3} GeV with the same coding.

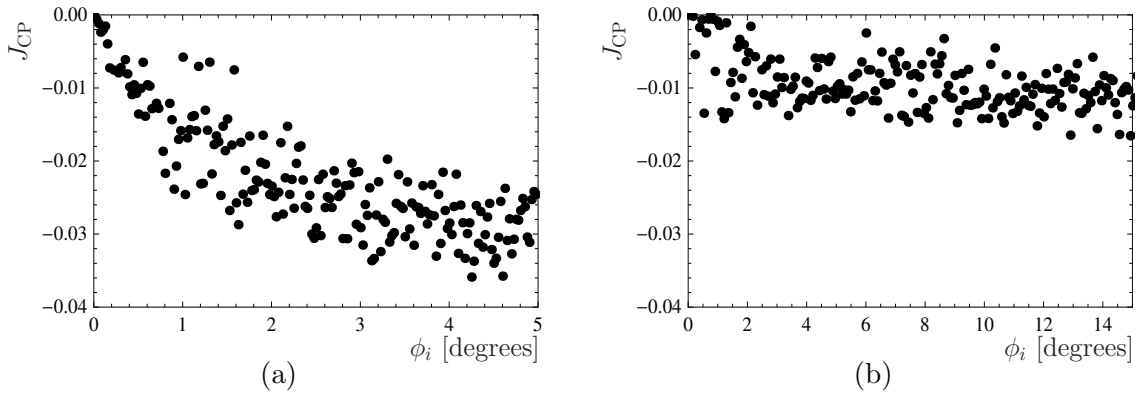

Figure 3: $J_{\rm CP}$ as a function $\phi := \phi_1 = \phi_2 = \phi_3$ in degrees for (a) P_1 and (b) P_2.

As an example we give in Fig. 2 the adjustment of v_i and the absolute values of ϵ_i as a function of the phases $\phi_i = \arctan\left(\epsilon_i^I/\epsilon_i^R\right)$ for the case P_2. Here and in the following we will take the phases of all three ϵ_i to be equal to maximize the effects. The width of the bands reflects the experimental uncertainty of the neutrino data and the upper bound of the complex phases is given by the requirement to obtain correctly both neutrino mass scales at the same time. In principle one could get a somewhat larger range be adjusting the soft parameters in the sbottom and in the stau sector [32, 36]. However, as no new features show up for larger

values of the complex phases we do not pursue this road. This can also be seen by checking the Jarlskog invariant $J_{\rm CP}$ of the PMNS-matrix defined in Eq. (20) which we show in Fig. 3. Taking the current neutrino data leads to an upper bound $|J_{\rm CP}| \leq 0.040$ assuming a maximal Dirac phase. Note, that we reach this bound in case of scenario P_1.

3.2 Decay of the LSP

The smallness of the neutrino masses and in turn the smallness of the BRpV parameters imply a small decay width of the neutralino, such that it decays out of equilibrium in the early universe. Additionally the decays come with displaced vertices in collider experiments [59–61] allowing an experimental verification of this feature at the LHC. Taking the real values for the R-parity breaking parameters as provided in Tab. 1 we find for scenario P_1 at NLO

$$\Gamma\left(\tilde{\chi}_1^0 \to e^\pm W^\mp\right) = 3.36 \cdot 10^{-16}\ \text{GeV}, \qquad \Gamma\left(\tilde{\chi}_1^0 \to \mu^\pm W^\mp\right) = 1.31 \cdot 10^{-14}\ \text{GeV} \tag{33}$$

$$\Gamma\left(\tilde{\chi}_1^0 \to \tau^\pm W^\mp\right) = 1.44 \cdot 10^{-14}\ \text{GeV}, \qquad \Gamma\left(\tilde{\chi}_1^0 \to \nu_3(\overline{\nu}_3) Z\right) = 3.27 \cdot 10^{-15}\ \text{GeV} \tag{34}$$

and for scenario P_2 accordingly

$$\Gamma\left(\tilde{\chi}_1^0 \to e^\pm W^\mp\right) = 3.07 \cdot 10^{-16}\ \text{GeV}, \qquad \Gamma\left(\tilde{\chi}_1^0 \to \mu^\pm W^\mp\right) = 7.71 \cdot 10^{-15}\ \text{GeV} \tag{35}$$

$$\Gamma\left(\tilde{\chi}_1^0 \to \tau^\pm W^\mp\right) = 1.04 \cdot 10^{-14}\ \text{GeV}, \qquad \Gamma\left(\tilde{\chi}_1^0 \to \nu_3(\overline{\nu}_3) Z\right) = 2.35 \cdot 10^{-15}\ \text{GeV} \quad . \tag{36}$$

scenario	P_1	P_2	P_1'
ϵ_1 [GeV]	$3.12 \cdot 10^{-2}$	$2.21 \cdot 10^{-2}$	$2.62 \cdot 10^{-2}$
ϵ_2 [GeV]	$3.13 \cdot 10^{-2}$	$2.22 \cdot 10^{-2}$	$2.62 \cdot 10^{-2}$
ϵ_3 [GeV]	$-3.13 \cdot 10^{-2}$	$-2.22 \cdot 10^{-2}$	$-2.62 \cdot 10^{-2}$
v_1 [GeV]	$-1.45 \cdot 10^{-3}$	$-1.20 \cdot 10^{-4}$	$-1.23 \cdot 10^{-3}$
v_2 [GeV]	$-1.27 \cdot 10^{-3}$	$7.70 \cdot 10^{-6}$	$-1.05 \cdot 10^{-3}$
v_3 [GeV]	$1.71 \cdot 10^{-3}$	$3.40 \cdot 10^{-4}$	$1.43 \cdot 10^{-3}$

Table 1: Standard choice of real R-parity violating parameters for the three scenarios such that neutrino data [22] are correctly explained.

The final states $e^\pm W^\mp$ have considerably smaller decay widths than the others, the reason being the generation of the atmospheric scale of neutrino mixing at tree-level. The decays in the two lightest neutrino flavors are both vanishing at tree-level [62], but also at loop-level. Due to $\Gamma < H(T = m_{\tilde{\chi}_1^0}) \approx 2 \cdot 10^{-14}\,\text{GeV}$ the decay of the lightest neutralino at the temperature $T = m_{\tilde{\chi}_1^0}$ occurs out of equilibrium. Further details with respect to the out-of-equilibrium decay can be found in the subsequent section. We emphasize that an out-of-equilibrium decay only occurs for a light neutralino $m_{\tilde{\chi}_1^0} \lesssim 100\,\text{GeV}$. For heavier neutralinos $\gtrsim 150\,\text{GeV}$ the decay widths start to exceed the Hubble parameter. Only a detailed description with Boltzmann equations can reveal the impact on lepton and baryon asymmetries.

Before presenting our results for the particle densities in the early universe, let us briefly mention the effects of the complex phases ϕ_i on the partial decay widths and the individual

CP asymmetries, the latter being defined as

$$\delta_\Gamma = \frac{\Gamma^+ - \Gamma^-}{\Gamma^+ + \Gamma^-} \tag{37}$$

with $\Gamma^\pm = \Gamma(\tilde{\chi}_1^0 \to l^\pm W^\mp)$ or $\Gamma^\pm = \Gamma(\tilde{\chi}_1^0 \to \nu(\overline{\nu})Z)$. For both scenarios P_1 and P_2 Fig. 4 shows the decay widths Γ^+ of the LSP in GeV for the various decay channels. The CP asymmetry δ_Γ is presented in Fig. 5 for both scenarios: The CP violation in the final state involving electrons is effectively of the same size as in the other decay channels, if one takes into account the smallness of the decay widths in this particular final state. Changing the sign $\sin\phi_i \to -\sin\phi_i$ for all $i \in \{1,2,3\}$ yields $\delta_\Gamma \to -\delta_\Gamma$.

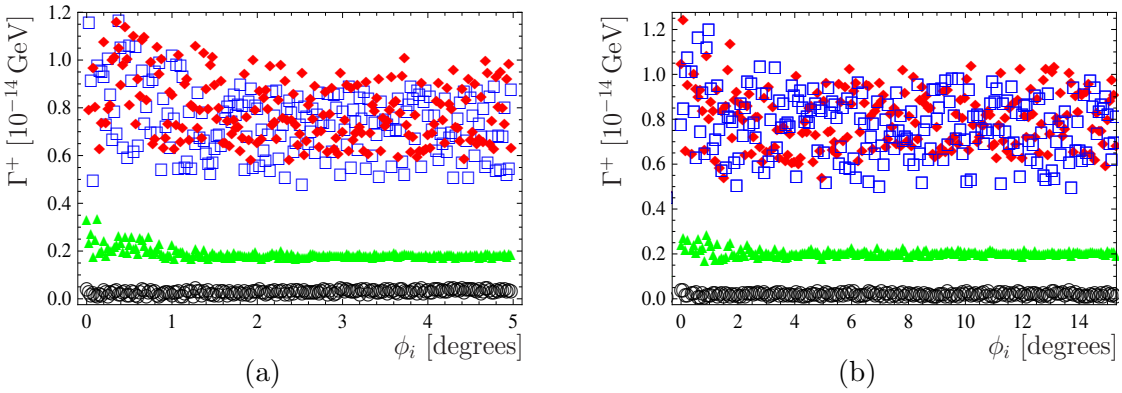

Figure 4: Decay widths Γ^+ for the final states e^+W^- (black, circle), μ^+W^- (blue, square), τ^+W^- (red, diamond), $\bar{\nu}_3 Z$ (green, triangle) as a function of $\phi := \phi_1 = \phi_2 = \phi_3$ in degrees for (a) P_1 and (b) P_2.

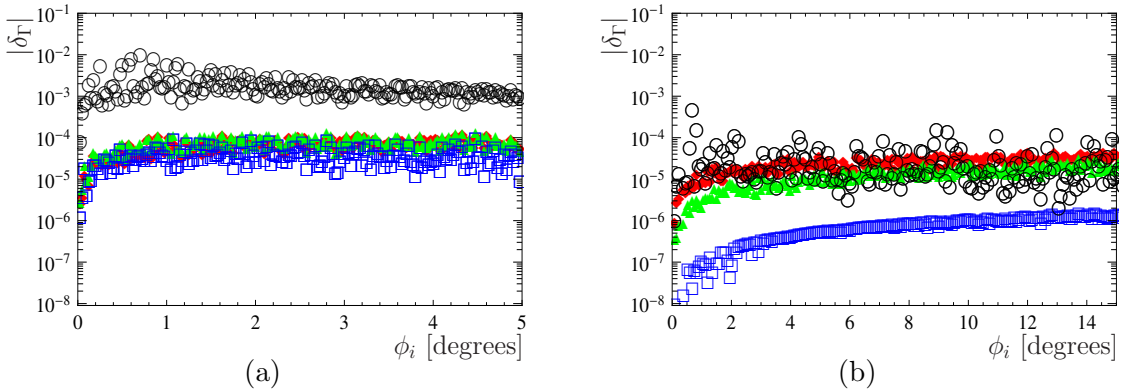

Figure 5: CP asymmetry $|\delta_\Gamma|$ for the final states $e^\pm W^\mp$ (black, circle), $\mu^\pm W^\mp$ (blue, square), $\tau^\pm W^\mp$ (red, diamond), $\nu_3(\bar{\nu}_3)Z$ (green, triangle) defined in Eq. (37) as a function of $\phi := \phi_1 = \phi_2 = \phi_3$ in degrees for (a) P_1 and (b) P_2.

In order to estimate the size of the asymmetry in decays $\tilde{\chi}_1^0 \to \nu(\bar{\nu})h$ we add a scenario P_1', where the gaugino mass M_1 is shifted from 100 GeV to 150 GeV, such that the decay channel into the light Higgs h opens. A possible set of R-parity violating parameters fulfilling neutrino data is added to Tab. 1 and Fig. 6 presents the corresponding CP asymmetries. The CP asymmetry in the final state $\nu_3(\bar{\nu}_3)h$ is of a similar size as in case of the final states with

gauge boson, whereas the ones in the first two neutrino mass generations are negligible. The $\nu_i(\bar{\nu}_i)h$ final states have branching fractions comparable to $\mu^\pm/\tau^\pm W^\mp$ final states and thus their inclusion for $m_{\tilde{\chi}_1^0} > m_h$ is advisable.

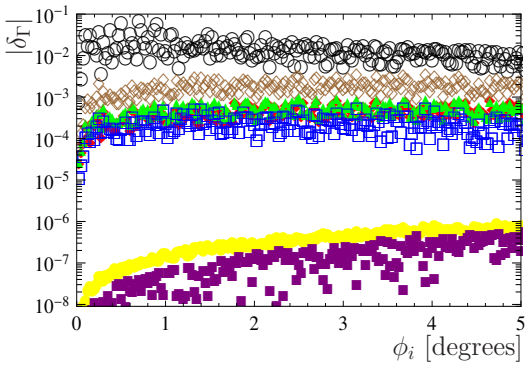

Figure 6: CP asymmetry $|\delta_\Gamma|$ for the final states $e^\pm W^\mp$ (black, empty circle), $\mu^\pm W^\mp$ (blue, empty square), $\tau^\pm W^\mp$ (red, filled diamond), $\nu_3(\bar{\nu}_3)Z$ (green, filled triangle), $\nu_1(\bar{\nu}_1)h$ (yellow, filled circle), $\nu_2(\bar{\nu}_2)h$ (purple, filled square) and $\nu_3(\bar{\nu}_3)h$ (brown, empty triangle) defined in Eq. (37) as a function of $\phi := \phi_1 = \phi_2 = \phi_3$ in degrees for P_1'.

3.3 Lepton asymmetries in the CP conserving BRpV

In this subsection we discuss the effect of the LSP decays on the number densities and thus the lepton and baryon asymmetries in the early universe and we start with the case of CP conserving BRpV. The small decay rates of the neutralino can have a sizable impact on lepton asymmetries, which could for example be generated at an earlier stage of the universe by the Affleck-Dine mechanism [14]. If for the moment we ignore neutrino data and choose all decay widths slightly larger than the Hubble parameter $\Gamma > H(T = m_{\tilde{\chi}_1^0})$, a sizable wash-out of initial lepton asymmetries can occur [63]. This is explicitly demonstrated in Fig. 7, where all widths are set to $5 \cdot 10^{-14}$ GeV and the annihilation cross sections are taken from scenario P_2. For a light neutralino $m_{\tilde{\chi}_1^0} < T_c$ initial baryon asymmetries are only mildly affected, since for $T < T_c$ they are decoupled from the lepton asymmetries - see Sect. 3.4. For numerical stability we choose all initial particle densities equal to their equilibrium density with (small) displacements to establish the shown asymmetries. The presented effects are independent of the sign of the initial lepton asymmetry δ_N. Fig. 7 (b) shows the behaviour of the LSP number density, which follows the equilibrium density and thus motivates the neglect of scattering processes.

In accordance to Refs. [64, 65] the wash-out of an initial asymmetry driven by the back-reaction of leptons, quarks, neutrinos and their antiparticles to the LSP and the decays of the LSP itself stays small, if just one of the flavor final states is suppressed with respect to the others and thus decays out of equilibrium. To confirm this statement Fig. 8 shows the small wash-out for different initial lepton asymmetries for both scenarios P_1 and P_2 with fulfilled neutrino data. Initially present lepton and thus also baryon asymmetries are almost conserved, if neutrino data is explained by the BRpV parameters.

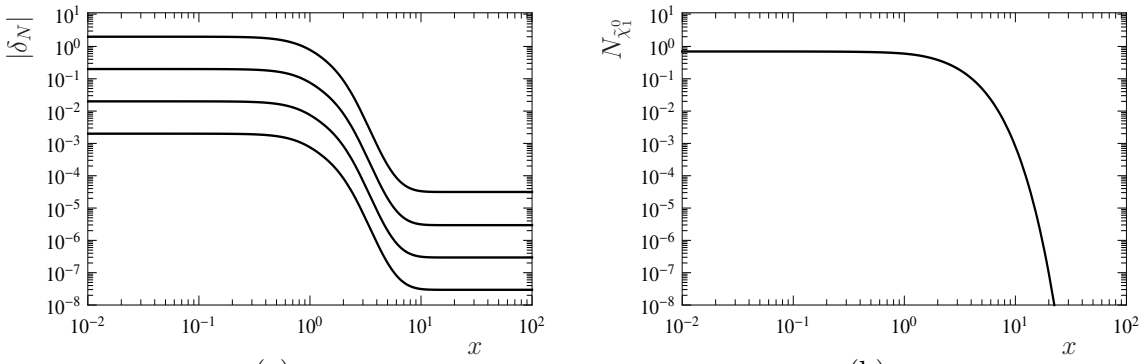

Figure 7: (a) Lepton asymmetry $|\delta_N|$ as defined in Eq. (29) as a function of x for CP conserving BRpV for all widths set to $5 \cdot 10^{-14}$ GeV for different asymmetries δ_N at $x = 10^{-2}$; (b) LSP density as a function of x for the same cases.

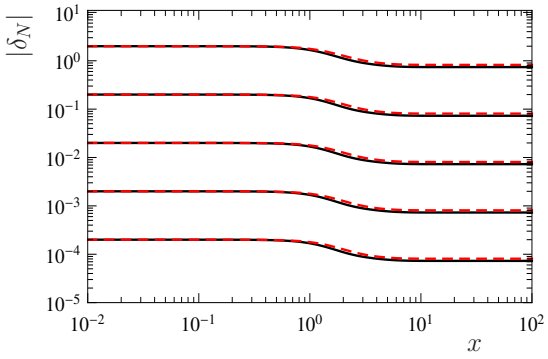

Figure 8: Lepton asymmetry $|\delta_N|$ as defined in Eq. (29) as a function of x for CP conserving BRpV for P_1 (black) and P_2 (red, dashed) for different asymmetries δ_N at $x = 10^{-2}$.

3.4 Baryogenesis via Leptogenesis in the CP violating BRpV

In this subsection we discuss the impact of CP violation by complex BRpV parameters ϵ_i on the decay widths of the lightest neutralino and the lepton and baryon asymmetries in the early universe. Before doing so let us briefly comment on the stringent bounds coming from the non-observation of electric dipole-moments, in particular the one of the electron has to be below $\lesssim 10^{-28}$ ecm [66]. As we only consider CP phases in the R-parity violating parameters, the corresponding effect is small and in case of the slepton and sneutrino contributions further suppressed by their heavy masses. The potentially most troublesome are the $\tilde{\chi}^0_j$-W contributions which are proportional to $\mathrm{Im}(O^W_{Lej}(O^W_{Rej})^*)$. Using an expansion in the R-parity violating parameters [40, 62] one finds that this product is tiny for several reasons: (i) it is proportional to the R-parity violation couplings squared, (ii) it is suppressed by a factor $Y^{11}_E v_d/\min(\mu, M_2)$ and (iii) it vanishes completely in case of a pure bino. Numerically we find that the induced electron dipole-moment is always below $\mathcal{O}(10^{-32}$ ecm) in our examples.

For relatively large phases ϕ_i and thus CP asymmetries up to per-mile level the CP violating

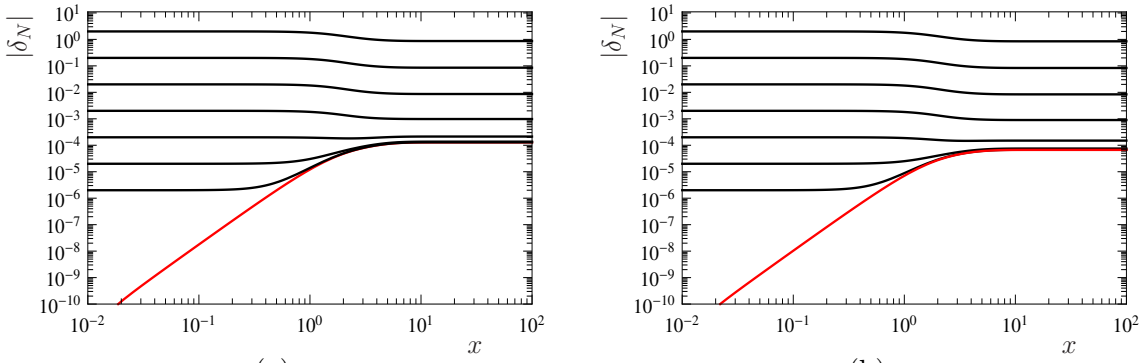

Figure 9: Lepton asymmetry $|\delta_N|$ as defined in Eq. (29) for (a) P_1 with phase $\phi := \phi_1 = \phi_2 = \phi_3 = 5$ degrees; (b) P_2 with phase $\phi := \phi_1 = \phi_2 = \phi_3 = 15$ degrees in both cases for different initial asymmetries δ_N at $x = 10^{-2}$.

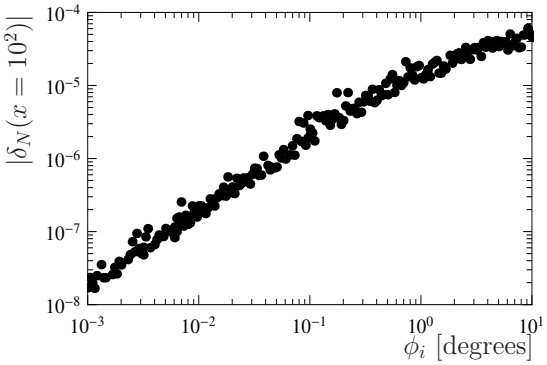

Figure 10: Resulting lepton asymmetry $|\delta_N|$ at $x = 10^2$ as a function of $\phi := \phi_1 = \phi_2 = \phi_3$ for P_2 for zero initial asymmetry $\delta_N = 0$ at $x = 10^{-2}$.

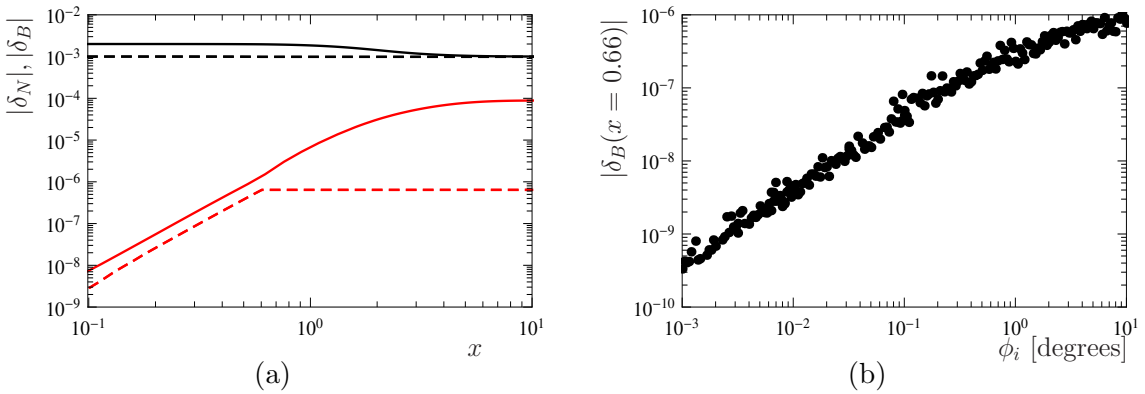

Figure 11: (a) Lepton asymmetry $|\delta_N|$ (solid) and baryon asymmetry $|\delta_B|$ (dashed) for scenario P_2 with phase $\phi := \phi_1 = \phi_2 = \phi_3 = 15$ degrees for two different initial asymmetries δ_N, δ_B at $x = 10^{-2}$; (b) Resulting baryon asymmetry $|\delta_B(x = 0.66)|$ as a function of $\phi := \phi_1 = \phi_2 = \phi_3$ for P_2 for zero initial asymmetry $\delta_N = \delta_B = 0$ at $x = 10^{-2}$.

contributions can have sizable effects on lepton asymmetries in the universe. If the initial lepton asymmetry δ_N is large, the effect of the BRpV induced wash-out dominates - as discussed in the previous subsection. But for initial lepton asymmetries being rather small $|\delta_N| < 10^{-5}$ the CP violating contributions to the LSP decays come into the game. They induce a lepton asymmetry of $|\delta_N| \sim 10^{-5} - 10^{-3}$, if the complex phases ϕ_i are chosen large ~ 1 degree. Details can be taken from Fig. 9 for scenario P_1 choosing a phase of 5 degrees and scenario P_2 with a phase of 15 degrees. Fig. 10 shows the obtained lepton asymmetry in the universe as a function of the CP phases ϕ_i in the BRpV parameters for scenario P_2, if initially no lepton asymmetry is present $\delta_N(x = 10^{-2}) = 0$.

As pointed out in the previous section $\sin\phi_i \to -\sin\phi_i$ for all $i \in \{1, 2, 3\}$ results in $\delta_\Gamma \to -\delta_\Gamma$, which induces $\delta_N \to -\delta_N$, if no initial asymmetry is present. This statement implies, that for different signs in $\sin\phi_i$ also smaller lepton asymmetries with different signs for the three generations can be accommodated. Additionally a cancellation between existing lepton asymmetries and the generated lepton asymmetries can be arranged.

As discussed in Sect. 2.4 we add sphaleron transitions to our Boltzmann equations in order to determine the baryon asymmetry generated from the lepton asymmetry and vice versa. We therefore start once with initial and once without initial lepton and baryon asymmetries and examine how both evolve as a function of the temperature parameterized by x. Fig. 11 (a) shows the corresponding results for P_2 again for a phase of $\phi := \phi_1 = \phi_2 = \phi_3 = 15$ degrees. For numerical stability we choose $\delta_B = -\eta(x)\delta_L$ at $x = 10^{-2}$ in case of given initial asymmetries. As expected, the baryon asymmetry δ_B freezes at temperatures $x = m_{\tilde{\chi}_1^0}/T_c \approx 0.66$, whereas the lepton asymmetry δ_N evolves further driven by the neutralino decays. Thus, if an initial baryon asymmetry is present, it is hardly affected by CP violating decays of light neutralinos. The reason is, that for $x \gtrsim 0.66$, where the change of the lepton asymmetry is strongest, the sphaleron process is close to be frozen out. On the other hand, even in case of no initial baryon asymmetry it can be generated at small x. We translate Fig. 10 to the corresponding baryon asymmetry obtained at $x \approx 0.66$ and present the result in Fig. 11 (b). Since the baryon asymmetry remains constant for lower temperatures, it yields $\delta_B(x = 10^2) = \delta_B(x = 0.66)$. A baryon asymmetry of order 10^{-10} as observed in the universe can be generated from neutralino decays having a mass of $m_{\tilde{\chi}_1^0} \sim 100\,\text{GeV}$ in BRpV in case of rather small complex phases $\phi_i \sim 10^{-3}$ degrees for the R-parity breaking parameters. The generated lepton asymmetry is approximately two orders of magnitude larger. Alternatively larger phases are possible, if a cancellation between various CP violating contributions occurs.

3.5 LSP annihilation to SM particles

As it was pointed out in Ref. [17] R-parity conserving scattering processes, which lead to an annihilation of the LSP, can impact on the densities of the LSP and the SM particles. Therefore all our discussion included the R-parity conserving annihilation processes. Within this section we want to discuss their impact in more detail, neglecting sphaleron transitions for simplicity. For scenario P_2 Fig. 12 (a) shows the thermally averaged cross sections $\langle\sigma_{ij}v\rangle$ for different final states in $1/\text{GeV}^2$ as obtained by `micrOMEGAs`. Fig. 12 (b) presents for comparison $\hat{\sigma}(\tilde{\chi}_1^0\tilde{\chi}_1^0 \to b\bar{b})N^{eq,2}$ with N^{eq} being the neutralino equilibrium density versus $\text{K}_1/\text{K}_2 N^{eq}\Gamma$ with $\Gamma = 10^{-14}$ GeV and the ratio K_1/K_2 of modified Bessel functions and thus

reflects the right-hand side terms entering the Boltzmann equations Eq. (26). The annihilation processes dominate the evolution of the Boltzmann equations for most temperatures, their relative importance drops below the decay processes only for very low temperatures $T < m_{\tilde{\chi}_1^0}$.

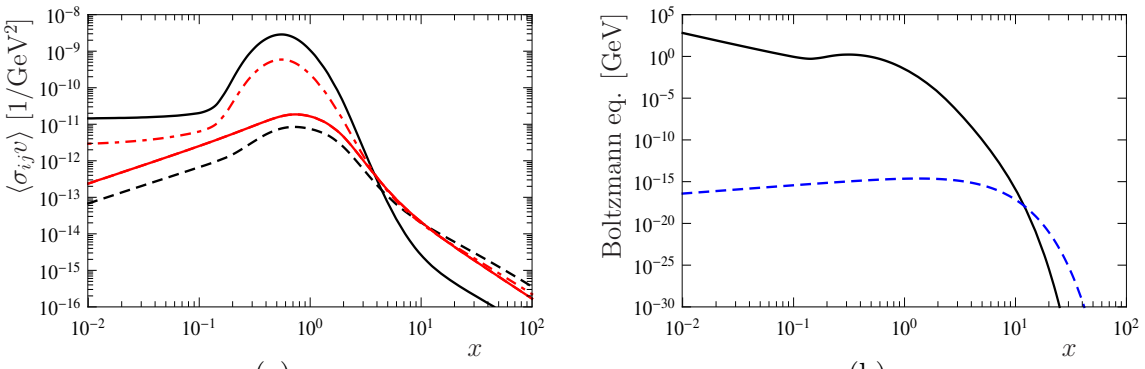

Figure 12: (a) Cross section $\langle\sigma_{ij}v\rangle$ in 1/GeV^2 as a function of x for P_2 for different final states: $ij = d\bar{d}/s\bar{s}/b\bar{b}$ (black), $u\bar{u}/c\bar{c}/t\bar{t}$ (black, dashed), $\tau^+\tau^-$ (red, dot-dashed), $e^+e^-/\mu^+\mu^-$ (red); (b) $K_1/K_2 N^{eq}\Gamma$ in GeV with $\Gamma = 10^{-14}$ GeV (blue, dashed) and $\hat{\sigma}(\tilde{\chi}_1^0\tilde{\chi}_1^0 \to b\bar{b})N^{eq,2}$ in GeV (black) as a function of x.

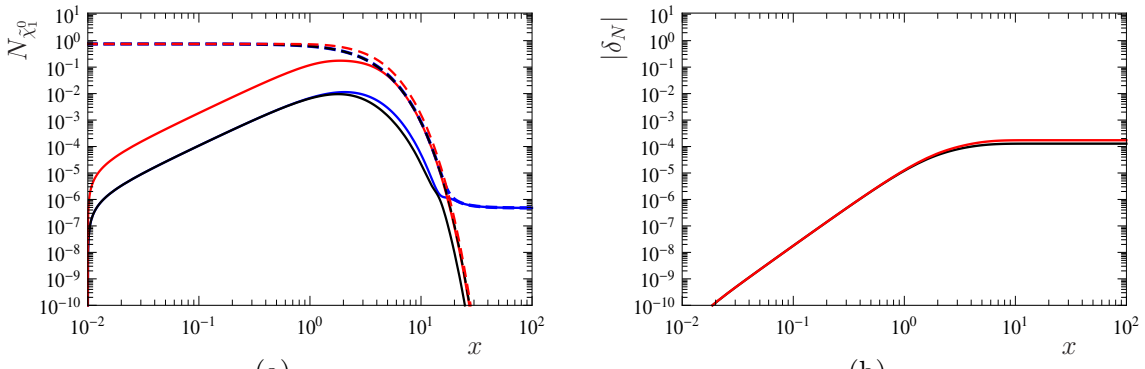

Figure 13: (a) LSP number density $|N_{\tilde{\chi}_1^0} - N^{eq}_{\tilde{\chi}_1^0}|$ (solid) and $N_{\tilde{\chi}_1^0}$ (dashed) as a function of x for only annihilation (blue), only decays (red), annihilation and decays (black) for P_1 with phase $\phi_i = 5$ degrees; (b) Evolution of δ_N as defined in Eq. (29) as a function of x for only decays (red), annihilation and decays (black) for the same case.

The impact of the annihilation versus the decay processes in the Boltzmann equations is further elaborated in Fig. 13 for scenario P_1. Scenario P_2 is visually indistinguishable from P_1. The left Fig. 13 (a) shows the neutralino density $N_{\tilde{\chi}_1^0}$ and its difference to the corresponding equilibrium value $|N_{\tilde{\chi}_1^0} - N^{eq}_{\tilde{\chi}_1^0}|$ for three different scenarios: In case of only annihilation processes, which corresponds to a scenario of the MSSM with R-parity conservation, the well-known freeze-out of the lightest SUSY particle yielding a constant neutralino density is observed at low temperatures. If just CP violating decays of the neutralinos are included, the neutralino density vanishes for large x. In case of annihilation and decay processes the

neutralino density closely follows the case of only annihilation processes, but all neutralinos tend to decay at low temperatures.

The right Fig. 13 (b) presents the evolving lepton asymmetry, if no initial lepton asymmetry $\delta_N = 0$ at $x = 10^{-2}$ is assumed. A difference between just decay processes and decay as well as annihilation processes can be observed. However, the order of magnitude of the generated lepton asymmetry remains unchanged. The inclusion of sphaleron transitions will distort the observations only minimally.

4 Conclusion

We examined the effects of LSP decays, the LSP being a light neutralino $m_{\tilde{\chi}_1^0} \sim 100\,\text{GeV}$, in bilinear R-parity violation (BRpV) with complex BRpV parameters on the lepton and baryon asymmetries in the early universe. We presented a description of the neutralino sector at NLO for complex BRpV parameters and calculated the LSP decays at NLO. In this way we get both, the total width as well as the induced CP asymmetries between leptonic and antileptonic final states. With respect to the evolution of number densities in the early universe our discussion includes - apart from the mentioned LSP decays and their inverse counterparts - the LSP annihilation to SM particles, which we assume to be very close to the minimal supersymmetric standard model. In order to describe the transition between lepton and baryon asymmetries we add a simple description of sphaleron processes, which however get frozen out at the mass scale of the neutralino if its mass is below the electroweak phase transition.

Our conclusion is two-sided: Initial lepton and baryon asymmetries are preserved by the LSP decay, if neutrino data is described correctly by the BRpV parameters. On the other hand instead, lepton and baryon asymmetries can also be generated in the complex BRpV model, the latter being in accordance to the observation in our universe. Clearly, both statements hold for different values of the CP violating phases in case of a light neutralino LSP. Last but not least we note that in both regimes the via those couplings induced electric dipole-moment of the electron is well below the sensitivity of present and future experiments.

Acknowledgments We thank M. Hirsch and Th. Konstandin for discussions and U. Langenfeld for collaboration in the early stage of this project. This work is supported by the DFG, project no. PO-1337/2-1, and by the research training group GRK 1147. S. L. acknowledges support by the DFG through the SFB 676 "Particles, Strings and the Early Universe". S. L. was also supported by the DFG grant HA 2990/5-1.

A Formulas: Boltzmann equations

In this section we present the full set of Boltzmann equations for the neutralino and the final state particles resulting from the gauge bosons/Higgs decays namely leptons, neutrinos (antineutrinos) and quarks (antiquarks). To be brief we just add the decay mode $h \to q\bar{q}$ for the Higgs boson. Moreover to shorten the subsequent formulas, we leave the distinction of q_1 and q_2 to the reader. It is clear that e.g. the decays of the W boson involve two different quark types, whereas the decays of the Z boson result in identical quark types $q_i\bar{q}_i$. Accordingly Eq. (42) and Eq. (43) have to be doubled for both quarks q_1 and q_2. For details with respect to the sphaleron transitions we refer to Sect. 2.4. To shorten our notation we write $\Gamma, \mathrm{Br}(X|YZ) := \Gamma, \mathrm{Br}(X \to YZ)$ and $\hat{\sigma}(XX|YZ) := \hat{\sigma}(XX \to YZ)$. We also define $\widetilde{N}_X$ to be the ratio of the number density of the particle $X \in \{\ell_i^\pm, \nu, \bar{\nu}, q, \bar{q}\}$ and its value in the thermal equilibrium:

$$\widetilde{N}_X = \frac{N_X}{N_X^{eq}} \tag{38}$$

$$\begin{aligned}
xH\frac{dN_{\tilde{\chi}_1^0}}{dx} = &-\frac{\mathrm{K}_1(x)}{\mathrm{K}_2(x)}\sum_{i,j}\sum_{q,\bar{q}}\Big[N_{\tilde{\chi}_1^0}\Big(\Gamma(\tilde{\chi}_1^0|\ell_i^+W^-) + \Gamma(\tilde{\chi}_1^0|\ell_i^-W^+)\Big)\mathrm{Br}(W^\pm|\ell_j^\pm\nu(\bar{\nu})_j) \\
&- \widetilde{N}_{\ell_i^+}\widetilde{N}_{\ell_j^-}\widetilde{N}_{\bar{\nu}_j}N_{\tilde{\chi}_1^0}^{eq}\Gamma(\ell_i^+W^-|\tilde{\chi}_1^0)\mathrm{Br}(W^-|\ell_j^-\bar{\nu}_j) \\
&- \widetilde{N}_{\ell_i^-}\widetilde{N}_{\ell_j^+}\widetilde{N}_{\nu_j}N_{\tilde{\chi}_1^0}^{eq}\Gamma(\ell_i^-W^+|\tilde{\chi}_1^0)\mathrm{Br}(W^+|\ell_j^+\nu_j) \\
&+ N_{\tilde{\chi}_1^0}\Big(\Gamma(\tilde{\chi}_1^0|\ell_i^-W^+) + \Gamma(\tilde{\chi}_1^0|\ell_i^+W^-)\Big)\mathrm{Br}(W^\pm|q\bar{q}) \\
&- \widetilde{N}_q\widetilde{N}_{\bar{q}}N_{\tilde{\chi}_1^0}^{eq}\Big(\widetilde{N}_{\ell_i^-}\Gamma(\ell_i^-W^+|\tilde{\chi}_1^0) + \widetilde{N}_{\ell_i^+}\Gamma(l_i^+W^-|\tilde{\chi}_1^0)\Big)\mathrm{Br}(W^\pm|q\bar{q}) \\
&+ N_{\tilde{\chi}_1^0}\Big(\Gamma(\tilde{\chi}_1^0|Z\nu_i) + \Gamma(\tilde{\chi}_1^0|Z\bar{\nu}_i)\Big)\mathrm{Br}(Z|\ell_j^-\ell_j^+) \\
&- \widetilde{N}_{\ell_j^-}\widetilde{N}_{\ell_j^+}N_{\tilde{\chi}_1^0}^{eq}\Big(\widetilde{N}_{\nu_i}\Gamma(Z\nu_i|\tilde{\chi}_1^0) + \widetilde{N}_{\bar{\nu}_i}\Gamma(Z\bar{\nu}_i|\tilde{\chi}_1^0)\Big)\mathrm{Br}(Z|\ell_j^-\ell_j^+) \\
&+ N_{\tilde{\chi}_1^0}\Big(\Gamma(\tilde{\chi}_1^0|Z\nu_i) + \Gamma(\tilde{\chi}_1^0|Z\bar{\nu}_i)\Big)\mathrm{Br}(Z|q\bar{q}) \\
&- \widetilde{N}_q\widetilde{N}_{\bar{q}}N_{\tilde{\chi}_1^0}^{eq}\Big(\widetilde{N}_{\nu_i}\Gamma(Z\nu_i|\tilde{\chi}_1^0) + \widetilde{N}_{\bar{\nu}_i}\Gamma(Z\bar{\nu}_i|\tilde{\chi}_1^0)\Big)\mathrm{Br}(Z|q\bar{q}) \\
&+ N_{\tilde{\chi}_1^0}\Big(\Gamma(\tilde{\chi}_1^0|h\nu_i) + \Gamma(\tilde{\chi}_1^0|h\bar{\nu}_i)\Big)\mathrm{Br}(h|q\bar{q}) \\
&- \widetilde{N}_q\widetilde{N}_{\bar{q}}N_{\tilde{\chi}_1^0}^{eq}\Big(\widetilde{N}_{\nu_i}\Gamma(h\nu_i|\tilde{\chi}_1^0) + \widetilde{N}_{\bar{\nu}_i}\Gamma(h\bar{\nu}_i|\tilde{\chi}_1^0)\Big)\mathrm{Br}(h|q\bar{q}) \\
&+ N_{\tilde{\chi}_1^0}\Gamma(\tilde{\chi}_1^0|Z\nu_i)\mathrm{Br}(Z|\nu_j\bar{\nu}_j) - \widetilde{N}_{\nu_i}\widetilde{N}_{\nu_j}\widetilde{N}_{\bar{\nu}_j}N_{\tilde{\chi}_1^0}^{eq}\Gamma(Z\nu_i|\tilde{\chi}_1^0)\mathrm{Br}(Z|\nu_j\bar{\nu}_j) \\
&+ N_{\tilde{\chi}_1^0}\Gamma(\tilde{\chi}_1^0|Z\bar{\nu}_i)\mathrm{Br}(Z|\nu_j\bar{\nu}_j) - \widetilde{N}_{\bar{\nu}_i}\widetilde{N}_{\nu_j}\widetilde{N}_{\bar{\nu}_j}N_{\tilde{\chi}_1^0}^{eq}\Gamma(Z\bar{\nu}_i|\tilde{\chi}_1^0)\mathrm{Br}(Z|\nu_j\bar{\nu}_j)\Big] \\
&- \sum_i\sum_{q,\bar{q}}\Big[\hat{\sigma}(\tilde{\chi}_1^0\tilde{\chi}_1^0|\ell_i^+\ell_i^-)(N_{\tilde{\chi}_1^0}^2 - \widetilde{N}_{\ell_i^+}\widetilde{N}_{\ell_i^-}N_{\tilde{\chi}_1^0}^{eq2}) \\
&+ \hat{\sigma}(\tilde{\chi}_1^0\tilde{\chi}_1^0|\nu_i\bar{\nu}_i)(N_{\tilde{\chi}_1^0}^2 - \widetilde{N}_{\nu_i}\widetilde{N}_{\bar{\nu}_i}N_{\tilde{\chi}_1^0}^{eq2}) + \hat{\sigma}(\tilde{\chi}_1^0\tilde{\chi}_1^0|q\bar{q})(N_{\tilde{\chi}_1^0}^2 - \widetilde{N}_q\widetilde{N}_{\bar{q}}N_{\tilde{\chi}_1^0}^{eq2})\Big]
\end{aligned} \tag{39}$$

$$
\begin{aligned}
xH\frac{dN_{\nu_j}}{dx} = \frac{\mathrm{K}_1(x)}{\mathrm{K}_2(x)}\sum_i\sum_{q,\bar{q}}\Big[& N_{\tilde{\chi}_1^0}\Gamma(\tilde{\chi}_1^0|\ell_i^- W^+)\mathrm{Br}(W^+|\ell_j^+\nu_j) \\
& - \widetilde{N}_{\ell_i^-}\widetilde{N}_{\ell_j^+}\widetilde{N}_{\nu_j}N^{eq}_{\tilde{\chi}_1^0}\Gamma(\ell_i^- W^+|\tilde{\chi}_1^0)\mathrm{Br}(W^+|\ell_j^+\nu_j) \\
& + N_{\tilde{\chi}_1^0}\Gamma(\tilde{\chi}_1^0|Z\nu_j)\Big(\mathrm{Br}(Z|\ell_i^-\ell_i^+) + \mathrm{Br}(Z|\nu_i\bar{\nu}_i) + \mathrm{Br}(Z|q\bar{q})\Big) \\
& - \widetilde{N}_{\nu_j}\widetilde{N}_{\ell_i^-}\widetilde{N}_{\ell_i^+}N^{eq}_{\tilde{\chi}_1^0}\Gamma(Z\nu_j|\tilde{\chi}_1^0)\mathrm{Br}(Z|\ell_i^-\ell_i^+) - \widetilde{N}_{\nu_j}\widetilde{N}_q\widetilde{N}_{\bar{q}}N^{eq}_{\tilde{\chi}_1^0}\Gamma(Z\nu_j|\tilde{\chi}_1^0)\mathrm{Br}(Z|q\bar{q}) \\
& + N_{\tilde{\chi}_1^0}\Gamma(\tilde{\chi}_1^0|h\nu_j)\mathrm{Br}(h|q\bar{q}) - \widetilde{N}_{\nu_j}\widetilde{N}_q\widetilde{N}_{\bar{q}}N^{eq}_{\tilde{\chi}_1^0}\Gamma(h\nu_j|\tilde{\chi}_1^0)\mathrm{Br}(h|q\bar{q}) \\
& - \widetilde{N}_{\nu_j}\widetilde{N}_{\nu_i}\widetilde{N}_{\bar{\nu}_i}N^{eq}_{\tilde{\chi}_1^0}\Gamma(Z\nu_j|\tilde{\chi}_1^0)\mathrm{Br}(Z|\nu_i\bar{\nu}_i) \\
& + N_{\tilde{\chi}_1^0}\Gamma(\tilde{\chi}_1^0|Z\bar{\nu}_j)\mathrm{Br}(Z|\nu_i\bar{\nu}_i) - \widetilde{N}_{\bar{\nu}_j}\widetilde{N}_{\nu_i}\widetilde{N}_{\bar{\nu}_i}N^{eq}_{\tilde{\chi}_1^0}\Gamma(Z\bar{\nu}_j|\tilde{\chi}_1^0)\mathrm{Br}(Z|\nu_i\bar{\nu}_i) \\
& + N_{\tilde{\chi}_1^0}\Gamma(\tilde{\chi}_1^0|Z\nu_i)\mathrm{Br}(Z|\nu_j\bar{\nu}_j) - \widetilde{N}_{\nu_i}\widetilde{N}_{\nu_j}\widetilde{N}_{\bar{\nu}_j}N^{eq}_{\tilde{\chi}_1^0}\Gamma(Z\bar{\nu}_j|\tilde{\chi}_1^0)\mathrm{Br}(Z|\nu_i\bar{\nu}_i)\Big] \\
& + \frac{1}{2}\hat{\sigma}(\tilde{\chi}_1^0\tilde{\chi}_1^0|\nu_j\bar{\nu}_j)(N^2_{\tilde{\chi}_1^0} - \widetilde{N}_{\nu_j}\widetilde{N}_{\bar{\nu}_j}N^{eq2}_{\tilde{\chi}_1^0}) + \frac{\gamma(x)}{12}\Big[\delta_B + \eta(x)\delta_L\Big]
\end{aligned}
\tag{40}
$$

$$
\begin{aligned}
xH\frac{dN_{\bar{\nu}_j}}{dx} = \frac{\mathrm{K}_1(x)}{\mathrm{K}_2(x)}\sum_i\sum_{q,\bar{q}}\Big[& N_{\tilde{\chi}_1^0}\Gamma(\tilde{\chi}_1^0|\ell_i^+ W^-)\mathrm{Br}(W^-|\ell_j^-\bar{\nu}_j) \\
& - \widetilde{N}_{\ell_i^+}\widetilde{N}_{\ell_j^-}\widetilde{N}_{\bar{\nu}_j}N^{eq}_{\tilde{\chi}_1^0}\Gamma(\ell_i^+ W^-|\tilde{\chi}_1^0)\mathrm{Br}(W^-|\ell_j^-\bar{\nu}_j) \\
& + N_{\tilde{\chi}_1^0}\Gamma(\tilde{\chi}_1^0|Z\bar{\nu}_j)\Big(\mathrm{Br}(Z|\ell_i^-\ell_i^+) + \mathrm{Br}(Z|\nu_i\bar{\nu}_i) + \mathrm{Br}(Z|q\bar{q})\Big) \\
& - \widetilde{N}_{\bar{\nu}_j}\widetilde{N}_{\ell_i^-}\widetilde{N}_{\ell_i^+}N^{eq}_{\tilde{\chi}_1^0}\Gamma(Z\bar{\nu}_j|\tilde{\chi}_1^0)\mathrm{Br}(Z|\ell_i^-\ell_i^+) - \widetilde{N}_{\bar{\nu}_j}\widetilde{N}_q\widetilde{N}_{\bar{q}}N^{eq}_{\tilde{\chi}_1^0}\Gamma(Z\bar{\nu}_j|\tilde{\chi}_1^0)\mathrm{Br}(Z|q\bar{q}) \\
& + N_{\tilde{\chi}_1^0}\Gamma(\tilde{\chi}_1^0|h\bar{\nu}_j)\mathrm{Br}(h|q\bar{q}) - \widetilde{N}_{\bar{\nu}_j}\widetilde{N}_q\widetilde{N}_{\bar{q}}N^{eq}_{\tilde{\chi}_1^0}\Gamma(h\bar{\nu}_j|\tilde{\chi}_1^0)\mathrm{Br}(h|q\bar{q}) \\
& - \widetilde{N}_{\bar{\nu}_j}\widetilde{N}_{\nu_i}\widetilde{N}_{\bar{\nu}_i}N^{eq}_{\tilde{\chi}_1^0}\Gamma(Z\bar{\nu}_j|\tilde{\chi}_1^0)\mathrm{Br}(Z|\bar{\nu}_i\bar{\nu}_i) \\
& + N_{\tilde{\chi}_1^0}\Gamma(\tilde{\chi}_1^0|Z\nu_j)\mathrm{Br}(Z|\nu_i\bar{\nu}_i) - \widetilde{N}_{\nu_j}\widetilde{N}_{\nu_i}\widetilde{N}_{\bar{\nu}_i}N^{eq}_{\tilde{\chi}_1^0}\Gamma(Z\nu_j|\tilde{\chi}_1^0)\mathrm{Br}(Z|\nu_i\bar{\nu}_i) \\
& + N_{\tilde{\chi}_1^0}\Gamma(\tilde{\chi}_1^0|Z\bar{\nu}_i)\mathrm{Br}(Z|\nu_j\bar{\nu}_j) - \widetilde{N}_{\bar{\nu}_i}\widetilde{N}_{\nu_j}\widetilde{N}_{\bar{\nu}_j}N^{eq}_{\tilde{\chi}_1^0}\Gamma(Z\bar{\nu}_i|\tilde{\chi}_1^0)\mathrm{Br}(Z|\nu_i\bar{\nu}_i)\Big] \\
& + \frac{1}{2}\hat{\sigma}(\tilde{\chi}_1^0\tilde{\chi}_1^0|\nu_j\bar{\nu}_j)(N^2_{\tilde{\chi}_1^0} - \widetilde{N}_{\nu_j}\widetilde{N}_{\bar{\nu}_j}N^{eq2}_{\tilde{\chi}_1^0}) - \frac{\gamma(x)}{12}\Big[\delta_B + \eta(x)\delta_L\Big]
\end{aligned}
\tag{41}
$$

$$
\begin{aligned}
xH\frac{dN_q}{dx} = \frac{\mathrm{K}_1(x)}{\mathrm{K}_2(x)}\sum_i\sum_{\bar{q}}\Big[& N_{\tilde{\chi}_1^0}\Gamma(\tilde{\chi}_1^0|\ell_i^- W^+)\mathrm{Br}(W^+|q\bar{q}) \\
& - \widetilde{N}_{\ell_i^-}\widetilde{N}_q\widetilde{N}_{\bar{q}}N^{eq}_{\tilde{\chi}_1^0}\Gamma(\ell_i^- W^+|\tilde{\chi}_1^0)\mathrm{Br}(W^+|q\bar{q}) + N_{\tilde{\chi}_1^0}\mathrm{Br}(Z|q\bar{q})\Big(\Gamma(\tilde{\chi}_1^0|Z\nu_i)+\Gamma(\tilde{\chi}_1^0|Z\bar{\nu}_i)\Big) \\
& - \widetilde{N}_q\widetilde{N}_{\bar{q}}N^{eq}_{\tilde{\chi}_1^0}\mathrm{Br}(Z|q\bar{q})\Big(\widetilde{N}_{\nu_i}\Gamma(Z\nu_i|\tilde{\chi}_1^0)+\widetilde{N}_{\bar{\nu}_i}\Gamma(Z\bar{\nu}_i|\tilde{\chi}_1^0)\Big) \\
& + N_{\tilde{\chi}_1^0}\mathrm{Br}(h|q\bar{q})\Big(\Gamma(\tilde{\chi}_1^0|h\nu_i)+\Gamma(\tilde{\chi}_1^0|h\bar{\nu}_i)\Big) \\
& - \widetilde{N}_q\widetilde{N}_{\bar{q}}N^{eq}_{\tilde{\chi}_1^0}\mathrm{Br}(h|q\bar{q})\Big(\widetilde{N}_{\nu_i}\Gamma(h\nu_i|\tilde{\chi}_1^0)+\widetilde{N}_{\bar{\nu}_i}\Gamma(h\bar{\nu}_i|\tilde{\chi}_1^0)\Big)\Big] \\
& + \sum_{\bar{q}}\Big[\frac{1}{2}\hat{\sigma}(\tilde{\chi}_1^0\tilde{\chi}_1^0|q\bar{q})(N^2_{\tilde{\chi}_1^0}-\widetilde{N}_q\widetilde{N}_{\bar{q}}N^{eq2}_{\tilde{\chi}_1^0})\Big] + \frac{\gamma(x)}{4}\Big[\delta_B+\eta(x)\delta_L\Big]
\end{aligned} \tag{42}
$$

$$
\begin{aligned}
xH\frac{dN_{\bar{q}}}{dx} = \frac{\mathrm{K}_1(x)}{\mathrm{K}_2(x)}\sum_i\sum_{q}\Big[& N_{\tilde{\chi}_1^0}\Gamma(\tilde{\chi}_1^0|\ell_i^+ W^-)\mathrm{Br}(W^-|q\bar{q}) \\
& - \widetilde{N}_{\ell_i^+}\widetilde{N}_q\widetilde{N}_{\bar{q}}N^{eq}_{\tilde{\chi}_1^0}\Gamma(\ell_i^+ W^-|\tilde{\chi}_1^0)\mathrm{Br}(W^-|q\bar{q}) + N_{\tilde{\chi}_1^0}\mathrm{Br}(Z|q\bar{q})\Big(\Gamma(\tilde{\chi}_1^0|Z\nu_i)+\Gamma(\tilde{\chi}_1^0|Z\bar{\nu}_i)\Big) \\
& - \widetilde{N}_q\widetilde{N}_{\bar{q}}N^{eq}_{\tilde{\chi}_1^0}\mathrm{Br}(Z|q\bar{q})\Big(\widetilde{N}_{\nu_i}\Gamma(Z\nu_i|\tilde{\chi}_1^0)+\widetilde{N}_{\bar{\nu}_i}\Gamma(Z\bar{\nu}_i|\tilde{\chi}_1^0)\Big) \\
& + N_{\tilde{\chi}_1^0}\mathrm{Br}(h|q\bar{q})\Big(\Gamma(\tilde{\chi}_1^0|h\nu_i)+\Gamma(\tilde{\chi}_1^0|h\bar{\nu}_i)\Big) \\
& - \widetilde{N}_q\widetilde{N}_{\bar{q}}N^{eq}_{\tilde{\chi}_1^0}\mathrm{Br}(h|q\bar{q})\Big(\widetilde{N}_{\nu_i}\Gamma(h\nu_i|\tilde{\chi}_1^0)+\widetilde{N}_{\bar{\nu}_i}\Gamma(h\bar{\nu}_i|\tilde{\chi}_1^0)\Big)\Big] \\
& + \sum_{q}\Big[\frac{1}{2}\hat{\sigma}(\tilde{\chi}_1^0\tilde{\chi}_1^0|q\bar{q})(N^2_{\tilde{\chi}_1^0}-\widetilde{N}_q\widetilde{N}_{\bar{q}}N^{eq2}_{\tilde{\chi}_1^0})\Big] - \frac{\gamma(x)}{4}\Big[\delta_B+\eta(x)\delta_L\Big]
\end{aligned} \tag{43}
$$

$$
\begin{aligned}
xH\frac{dN_{\ell_i^-}}{dx} = \frac{\mathrm{K}_1(x)}{\mathrm{K}_2(x)}\sum_j\sum_{q,\bar{q}}\Big[& N_{\tilde{\chi}_1^0}\Gamma(\tilde{\chi}_1^0|\ell_i^- W^+)\mathrm{Br}(W^+|\ell_j^+\nu_j) \\
& - \widetilde{N}_{\ell_i^-}\widetilde{N}_{\ell_j^+}\widetilde{N}_{\nu_j}N^{eq}_{\tilde{\chi}_1^0}\Gamma(\ell_i^- W^+|\tilde{\chi}_1^0)\mathrm{Br}(W^+|\ell_j^+\nu_j) \\
& + N_{\tilde{\chi}_1^0}\Gamma(\tilde{\chi}_1^0|\ell_i^- W^+)\mathrm{Br}(W^+|q\bar{q}) - \widetilde{N}_{\ell_i^-}\widetilde{N}_q\widetilde{N}_{\bar{q}}N^{eq}_{\tilde{\chi}_1^0}\Gamma(\ell_i^- W^+|\tilde{\chi}_1^0)\mathrm{Br}(W^+|q\bar{q}) \\
& + N_{\tilde{\chi}_1^0}\Gamma(\tilde{\chi}_1^0|\ell_j^+ W^-)\mathrm{Br}(W^-|\ell_i^-\bar{\nu}_i) - \widetilde{N}_{l_j^+}\widetilde{N}_{\ell_i^-}\widetilde{N}_{\bar{\nu}_i}N^{eq}_{\tilde{\chi}_1^0}\Gamma(l_j^+ W^-|\tilde{\chi}_1^0)\mathrm{Br}(W^-|\ell_i^-\bar{\nu}_i) \\
& + N_{\tilde{\chi}_1^0}\Gamma(\tilde{\chi}_1^0|Z\nu_j)\mathrm{Br}(Z|\ell_i^-\ell_i^+) - \widetilde{N}_{\nu_j}\widetilde{N}_{\ell_i^-}\widetilde{N}_{\ell_i^+}N^{eq}_{\tilde{\chi}_1^0}\Gamma(Z\nu_j|\tilde{\chi}_1^0)\mathrm{Br}(Z|\ell_i^-\ell_i^+) \\
& + N_{\tilde{\chi}_1^0}\Gamma(\tilde{\chi}_1^0|Z\bar{\nu}_j)\mathrm{Br}(Z|\ell_i^-\ell_i^+) - \widetilde{N}_{\bar{\nu}_j}\widetilde{N}_{\ell_i^-}\widetilde{N}_{\ell_i^+}N^{eq}_{\tilde{\chi}_1^0}\Gamma(Z\bar{\nu}_j|\tilde{\chi}_1^0)\mathrm{Br}(Z|\ell_i^-\ell_i^+)\Big] \\
& + \hat{\sigma}(\tilde{\chi}_1^0\tilde{\chi}_1^0|\ell_i^+\ell_i^-)(N^2_{\tilde{\chi}_1^0}-\widetilde{N}_{\ell_i^+}\widetilde{N}_{\ell_i^-}N^{eq2}_{\tilde{\chi}_1^0}) + \frac{\gamma(x)}{12}\Big[\delta_B+\eta(x)\delta_L\Big]
\end{aligned} \tag{44}
$$

$$
\begin{aligned}
xH\frac{dN_{\ell_i^+}}{dx} =& \frac{\mathrm{K}_1(x)}{\mathrm{K}_2(x)}\sum_j\sum_{q,\bar{q}}\Big[N_{\tilde{\chi}_1^0}\Gamma(\tilde{\chi}_1^0|\ell_i^+W^-)\mathrm{Br}(W^-|\ell_j^-\bar{\nu}_j) \\
&- \widetilde{N}_{l_i^+}\widetilde{N}_{\ell_j^-}\widetilde{N}_{\bar{\nu}_j}N^{eq}_{\tilde{\chi}_1^0}\Gamma(l_i^+W^-|\tilde{\chi}_1^0)\mathrm{Br}(W^-\to\ell_j^-\bar{\nu}_j) \\
&+ N_{\tilde{\chi}_1^0}\Gamma(\tilde{\chi}_1^0|\ell_i^+W^-)\mathrm{Br}(W^-|\bar{q}q) - \widetilde{N}_{\ell_i^+}\widetilde{N}_{\bar{q}}\widetilde{N}_q N^{eq}_{\tilde{\chi}_1^0}\Gamma(l_i^+W^-|\tilde{\chi}_1^0)\mathrm{Br}(W^-|\bar{q}q) \\
&+ N_{\tilde{\chi}_1^0}\Gamma(\tilde{\chi}_1^0|\ell_j^-W^+)\mathrm{Br}(W^+|\ell_i^+\nu_i) - \widetilde{N}_{\ell_j^-}\widetilde{N}_{l_i^+}\widetilde{N}_{\nu_i}N^{eq}_{\tilde{\chi}_1^0}\Gamma(\ell_j^-W^+|\tilde{\chi}_1^0)\mathrm{Br}(W^+|\ell_i^+\nu_i) \\
&+ N_{\tilde{\chi}_1^0}\Gamma(\tilde{\chi}_1^0|Z\nu_j)\mathrm{Br}(Z|\ell_i^-\ell_i^+) - \widetilde{N}_{\nu_j}\widetilde{N}_{\ell_i^-}\widetilde{N}_{\ell_i^+}N^{eq}_{\tilde{\chi}_1^0}\Gamma(Z\bar{\nu}_j|\tilde{\chi}_1^0)\mathrm{Br}(Z|\ell_i^-\ell_i^+) \\
&+ N_{\tilde{\chi}_1^0}\Gamma(\tilde{\chi}_1^0|Z\bar{\nu}_j)\mathrm{Br}(Z|\ell_i^-\ell_i^+) - \widetilde{N}_{\bar{\nu}j}\widetilde{N}_{\ell_i^-}\widetilde{N}_{\ell_i^+}N^{eq}_{\tilde{\chi}_1^0}\Gamma(Z\bar{\nu}_j|\tilde{\chi}_1^0)\mathrm{Br}(Z|\ell_i^-\ell_i^+)\Big] \\
&+ \hat{\sigma}(\tilde{\chi}_1^0\tilde{\chi}_1^0|\ell_i^+\ell_i^-)(N^2_{\tilde{\chi}_1^0} - \widetilde{N}_{\ell_i^+}\widetilde{N}_{\ell_i^-}N^{eq2}_{\tilde{\chi}_1^0}) - \frac{\gamma(x)}{12}\Big[\delta_B + \eta(x)\delta_L\Big] \qquad (45)
\end{aligned}
$$

References

[1] J. Beringer *et al.* [Particle Data Group Collaboration], Phys. Rev. D **86** (2012) 010001.

[2] C. J. Copi, D. N. Schramm and M. S. Turner, Science **267** (1995) 192 [astro-ph/9407006].

[3] E. W. Kolb and M. S. Turner, *The Early Universe*, (Addison-Wesley, Redwood City, CA, 1990)

[4] C. L. Bennett *et al.* [WMAP Collaboration], Astrophys. J. Suppl. **148** (2003) 1 [astro-ph/0302207].

[5] C. L. Bennett *et al.* [WMAP Collaboration], Astrophys. J. Suppl. **208** (2013) 20 [arXiv:1212.5225].

[6] A. D. Sakharov, Pisma Zh. Eksp. Teor. Fiz. **5** (1967) 32 [JETP Lett. **5** (1967) 24] [Sov. Phys. Usp. **34** (1991) 392] [Usp. Fiz. Nauk **161** (1991) 61].

[7] G. 't Hooft, Phys. Rev. D **14** (1976) 3432 [Erratum-ibid. D **18** (1978) 2199].

[8] M. Fukugita and T. Yanagida, Phys. Lett. B **174** (1986) 45.

[9] S. Y. Khlebnikov and M. E. Shaposhnikov, Nucl. Phys. B **308** (1988) 885.

[10] J. A. Harvey and M. S. Turner, Phys. Rev. D **42** (1990) 3344.

[11] P. D. Serpico and G. G. Raffelt, Phys. Rev. D **71** (2005) 127301 [astro-ph/0506162].

[12] V. Simha and G. Steigman, JCAP **0808** (2008) 011 [arXiv:0806.0179].

[13] L. A. Popa and A. Vasile, JCAP **0806** (2008) 028 [arXiv:0804.2971].

[14] I. Affleck and M. Dine, Nucl. Phys. B **249** (1985) 361.

[15] T. Hambye, E. Ma and U. Sarkar, Phys. Rev. D **62** (2000) 015010 [hep-ph/9911422].

[16] T. Hambye, E. Ma and U. Sarkar, Nucl. Phys. B **590** (2000) 429 [hep-ph/0006173].

[17] T. Hambye, Nucl. Phys. B **633** (2002) 171 [hep-ph/0111089].

[18] I. Ben-Dayan, hep-ph/0503232.

[19] J. Chakrabortty and S. Roy, Phys. Rev. D **85** (2012) 035014 [arXiv:1104.1387].

[20] D. V. Forero, M. Tortola and J. W. F. Valle, Phys. Rev. D **86** (2012) 073012 [arXiv:1205.4018].

[21] M. C. Gonzalez-Garcia, M. Maltoni, J. Salvado and T. Schwetz, JHEP **1212** (2012) 123 [arXiv:1209.3023].

[22] F. Capozzi *et al.*, Phys. Rev. D **89** (2014) 093018 [arXiv:1312.2878].

[23] D. V. Forero, M. Tortola and J. W. F. Valle, arXiv:1405.7540.

[24] R. Barbier *et al.*, Phys. Rept. **420**, 1 (2005) [hep-ph/0406039].

[25] M. Chemtob, Prog. Part. Nucl. Phys. **54** (2005) 71-191 [hep-ph/0406029].

[26] M. Hirsch and J. W. F. Valle, New J. Phys. **6**, 76 (2004) [hep-ph/0405015].

[27] R. Hempfling, Nucl. Phys. B **478** (1996) 3 [hep-ph/9511288].

[28] S. Roy and B. Mukhopadhyaya, Phys. Rev. **D55** (1997) 7020-7029 [hep-ph/9612447].

[29] M. A. Diaz, J. C. Romão and J. W. F. Valle, Nucl. Phys. **B524** (1998) 23-40 [hep-ph/9706315].

[30] M. Bisset, O. C. W. Kong, C. Macesanu and L. H. Orr, Phys. Lett. **B430** (1998) 274-280 [hep-ph/9804282].

[31] A. S. Joshipura and S. K. Vempati, Phys. Rev. **D60** (1999) 095009 [hep-ph/9808232].

[32] M. Hirsch *et al.*, Phys. Rev. D **62** (2000) 113008 [Erratum-ibid. D **65** (2002) 119901] [hep-ph/0004115].

[33] A. Abada, S. Davidson and M. Losada, Phys. Rev. **D65** (2002) 075010 [hep-ph/0111332].

[34] A. S. Joshipura, R. D. Vaidya and S. K. Vempati, Nucl. Phys. **B639** (2002) 290-306 [hep-ph/0203182].

[35] E. J. Chun, D. Jung and J. D. Park, Phys. Lett. **B557** (2003) 233-239 [hep-ph/0211310].

[36] M. A. Diaz *et al.*, Phys. Rev. D **68** (2003) 013009 [Erratum-ibid. D **71** (2005) 059904] [hep-ph/0302021].

[37] A. Dedes, S. Rimmer and J. Rosiek, JHEP **0608** (2006) 005 [hep-ph/0603225].

[38] M. Hirsch, T. Kernreiter and W. Porod, JHEP **0301** (2003) 034 [hep-ph/0211446].

[39] S. Liebler and W. Porod, Nucl. Phys. B **849** (2011) 213 [Erratum-ibid. B **856** (2012) 125] [arXiv:1011.6163].

[40] S. Liebler and W. Porod, Nucl. Phys. B **855** (2012) 774 [arXiv:1106.2921].

[41] L. J. Hall and M. Suzuki, Nucl. Phys. B **231**, 419 (1984).

[42] I-H. Lee, Phys. Lett. B **138** (1984) 121.

[43] I-H. Lee, Nucl. Phys. B **246** (1984) 120.

[44] G. G. Ross and J. W. F. Valle, Phys. Lett. B **151**, 375 (1985).

[45] J. R. Ellis *et al.*, Phys. Lett. B **150** (1985) 142.

[46] M. Nowakowski and A. Pilaftsis, Nucl. Phys. B **461** (1996) 19 [hep-ph/9508271].

[47] D. M. Pierce, J. A. Bagger, K. T. Matchev and R. Zhang, Nucl. Phys. B **491** (1997) 3 [hep-ph/9606211].

[48] B. O'Leary, W. Porod and F. Staub, JHEP **1205** (2012) 042 [arXiv:1112.4600].

[49] Z. Maki, M. Nakagawa and S. Sakata, Prog. Theor. Phys. **28** (1962) 870.

[50] C. Jarlskog, Phys. Rev. Lett. **55** (1985) 1039.

[51] W. Buchmüller, P. Di Bari and M. Plümacher, Annals Phys. **315** (2005) 305 [hep-ph/0401240].

[52] G. Belanger, F. Boudjema, A. Pukhov and A. Semenov, Comput. Phys. Commun. **174** (2006) 577 [hep-ph/0405253].

[53] G. Belanger, F. Boudjema, A. Pukhov and A. Semenov, Comput. Phys. Commun. **185** (2014) 960 [arXiv:1305.0237].

[54] M. D'Onofrio, K. Rummukainen and A. Tranberg, JHEP **1208** (2012) 123 [arXiv:1207.0685].

[55] M. D'Onofrio, K. Rummukainen and A. Tranberg, arXiv:1404.3565.

[56] G. Aad *et al.* [ATLAS Collaboration], JHEP **1406** (2014) 035 [arXiv:1404.2500].

[57] W. Porod, Comput. Phys. Commun. **153** (2003) 275 [hep-ph/0301101].

[58] W. Porod and F. Staub, Comput. Phys. Commun. **183** (2012) 2458 [arXiv:1104.1573].

[59] F. de Campos *et al.*, JHEP **0805** (2008) 048 [arXiv:0712.2156].

[60] F. De Campos *et al.*, Phys. Rev. D **82** (2010) 075002 [arXiv:1006.5075].

[61] F. de Campos *et al.*, Phys. Rev. D **86** (2012) 075001 [arXiv:1206.3605].

[62] W. Porod, M. Hirsch, J. Romão and J. W. F. Valle, Phys. Rev. D **63** (2001) 115004 [hep-ph/0011248].

[63] B. A. Campbell, S. Davidson, J. R. Ellis and K. A. Olive, Astropart. Phys. **1** (1992) 77.

[64] B. A. Campbell, S. Davidson, J. R. Ellis and K. A. Olive, Phys. Lett. B **297** (1992) 118 [hep-ph/9302221].

[65] A. G. Akeroyd, E. J. Chun, M. A. Diaz and D. Jung, Phys. Lett. B **582** (2004) 64 [hep-ph/0307385].

[66] J. Baron *et al.* [ACME Collaboration], Science **343** (2014) 6168, 269 [arXiv:1310.7534].